



Minireview/Hypothesis

## A knowledge-based three dimensional model of the Photosystem II reaction center of *Chlamydomonas reinhardtii*

Jin Xiong<sup>1,4</sup>, Shankar Subramaniam<sup>2,3</sup> & Govindjee<sup>1,2,\*,\*\*</sup>

<sup>1</sup>Department of Plant Biology, <sup>2</sup>Center for Biophysics and Computational Biology, and Department of Biochemistry, <sup>3</sup>Beckman Institute, University of Illinois at Urbana-Champaign, Urbana, IL 61801 USA; <sup>4</sup>Current address: Department of Biology, Indiana University, Bloomington, IN 47405 USA; \*Author for correspondence and reprints

Received 13 August 1997; accepted in revised form 25 February 1998

**Key words:** accessory chlorophylls, bicarbonate,  $\beta$ -carotene, computer-modelling, heme, manganese cluster, Photosystem II reaction center, reaction center chlorophyll P680

### Abstract

In this Minireview, a comparison of the binding niches of the PS II cofactors from several existing models of the PS II reaction center is provided. In particular, it discusses a three dimensional model of the Photosystem II (PS II) reaction center including D1, D2 and cytochrome *b559* proteins from the green alga *Chlamydomonas reinhardtii* that was specifically generated for this Minireview. This model is the most complete to date and includes accessory chlorophyll<sub>Z</sub>s, a manganese cluster, two molecules of  $\beta$ -carotene and cytochrome *b559*, all of which are essential components of the PS II reaction center. The modeling of the D1 and D2 proteins was primarily based on homology with the L and M subunits of the anoxygenic purple bacterial photosynthetic reaction centers. The non-homologous loop regions were built using a sequence specific approach by searching for the best-matched protein segments in the Protein Data Bank, and by imposing the matching conformations on the corresponding D1 and D2 regions. Cytochrome *b559* which is in close proximity to D1 and D2 was tentatively modeled in  $\alpha/\beta$  conformation and docked on the Q<sub>B</sub> side of the PS II reaction center according to experimental suggestions. An alternate docking on the Q<sub>A</sub> side is also shown for comparison. The cofactors in the PS II reaction center were modeled either by adopting the structures from the bacterial counterparts, when available, with modifications based on existing experimental data or by *de novo* modeling and docking in the most probable positions in the reaction center complex. The specific features of this model are the inclusion of the tetramanganese cluster (with calcium and chloride ions) in an open, C-shaped structure modeled within the D1/D2/cytochrome *b559* complex with D1-D170, D1-E189, D1-D342 and D1-A344 as putative ligands; and the modeling of two *cis*  $\beta$ -carotenes and two accessory chlorophyll<sub>Z</sub>s liganded by D1-H118 and D2-H117. We also analyzed residues in the model which may be involved in the D1 and D2 inter-protein interactions, as well as residues which may be involved in putative bicarbonate and water binding and transport.

**Abbreviations:** ABNR – adopted basis Newton Raphson energy minimization approach; BLAST – basic local alignment search tool; ENDOR – electron nuclear double resonance; EPR – electron paramagnetic resonance; ESE – electron spin echo; ESEEM – electron spin echo envelope modulation; P680 – the ‘special pair’ chlorophyll *a* and the primary electron donor of Photosystem II; PCC – Pasteur culture collection; PS II – Photosystem II; Q<sub>A</sub> – the primary plastoquinone electron acceptor of Photosystem II; Q<sub>B</sub> – the secondary plastoquinone electron acceptor of Photosystem II; rms – root mean square deviation

### Introduction

Photosystem II (PS II), one of the two photosystems in plants, algae, prochlorophytes and cyanobacteria,

\*\* The work was completed in 1997 when G was on sabbatical leave from the Department of Plant Biology, University of Illinois at Urbana-Champaign.

is the only protein complex in nature that is able to evolve molecular oxygen by oxidizing water (Debus 1992). The reaction center complex of PS II, where the photochemical reaction II takes place, consists of several membrane bound polypeptides including: D1, D2, a heterodimer of cytochrome *b559*, PsbI and PsbW (Vermaas et al. 1993; Diner and Babcock 1996; Nugent 1996). For a description of the genes and their expressions, see Herrmann et al. (1991). The reaction center, utilizing the harvested light energy, undergoes charge separation in picosecond time scale (Greenfield et al. 1997) followed by electron transfer from water to plastoquinone. Two major polypeptides of the reaction center, D1 and D2, contain a number of bound organic and inorganic cofactors that are crucial for the PS II photochemistry. These cofactors include a tetramanganese cluster, two redox active tyrosine residues labeled as Y<sub>Z</sub> and Y<sub>D</sub>, six chlorophyll *a* molecules, two pheophytins, and two plastoquinones. A non-heme iron, located between bound plastoquinones Q<sub>A</sub> and Q<sub>B</sub>, does not participate directly in the electron transfer but is vital for the electron transfer process. Bicarbonate anions are crucial for liganding to the non-heme iron and participating in the reduction of plastoquinone in PS II (Govindjee and van Rensen 1993). Two  $\beta$ -carotene molecules are present in the reaction center complex and are believed to be involved in a photoprotective process.

Despite the importance of this protein complex to provide electrons to Photosystem I and oxidize water to molecular oxygen, the molecular structure and the functional mechanism of the PS II reaction center are not yet fully understood. A high resolution X-ray crystal structure of the PS II reaction center is not yet available, only low resolution structures have been obtained (Rögner et al. 1996; Rhee et al. 1997). In the absence of the crystal structure of the PS II reaction center, much of the structural understanding of the PS II reaction center is derived from the significant sequence and functional homology with the non-oxygenic photosynthetic reaction centers of the purple non-sulfur bacteria *Rhodobacter (Rb.) sphaeroides* and *Rhodospseudomonas (Rps.) viridis*, for which high resolution crystal structures are available (Lancaster et al. 1995). A two-dimensional structure of plant Photosystem II at 8 Å resolution, reported by Rhee et al. (1997), confirms that the general feature of the PS II reaction center is homologous to the purple bacterial ones. This study, as well as previous studies on analysis of two-dimensional PS II crystal structures (Barber et al. 1997; Hankamer et al.

1997), confirmed that the PS II complex exists in a dimer form with a two-fold symmetry *in vivo*.

To aid in atomic level structural understanding of the PS II reaction center, several three dimensional computer models have been constructed based exclusively on the homology of D1/D2 polypeptides with the L/M subunits of the bacterial reaction center of *Rb. sphaeroides* and *Rps. viridis* (Trebst 1986; Bowyer et al. 1990; Svensson et al. 1990; Ruffle et al. 1992; Svensson et al. 1996; Xiong et al. 1996).

Though the comparison with the bacterial reaction centers is very useful, the PS II reaction center has several unique features that cannot be modeled directly by homology. Most of the previous models, based entirely on homology principle, are incomplete and fall short in predicting and analyzing features in PS II that are not found in the bacterial system. In order to construct a more reasonable and more useful computer model that includes specific features of the PS II reaction center, an approach combining homology and experimental knowledge is applied to model parts of the PS II reaction center which do not have counterparts in the bacterial reaction center. Based on the existing experimental knowledge of the structure and function of the PS II reaction center, molecular docking techniques, in association with other computational tools, were applied in modeling various possible conformations of the P680 chlorophylls, and bicarbonate anions (Ruffle and Nugent 1992; Ruffle et al. 1992; Xiong et al. 1996; Svensson et al. 1996). However, the tetramanganese cluster which is crucial for PS II oxygen evolution had not been included within the protein complex in most of the models. There have also been several other unique features of the PS II reaction center such as accessory chlorophyll<sub>z</sub>s (Koulougliotis et al. 1994), two  $\beta$ -carotene molecules (Kobayashi et al. 1990), and a conformation of the Q<sub>A</sub> pocket different from that in anoxygenic bacteria (Zheng and Dismukes 1996). All of these required further improvement from the previous models. There are also accumulating new experimental evidence regarding cytochrome *b559* which is an integral part of the PS II reaction center and that functions presumably in the process of photoprotection (Whitmarsh and Pakrasi 1996); this has provided sufficient information for a more complete, although still incomplete, molecular modeling of PS II.

In this Minireview, a comparison of the binding niches of the PS II cofactors from several existing models of the PS II reaction center is provided. In particular, we present here a more complete three dimensional model of the Photosystem II (PS II) reaction

center, including D1, D2 and cytochrome *b559* proteins from the unicellular green alga *Chlamydomonas reinhardtii*, that was specifically generated for this minireview. We chose to use *C. reinhardtii* because it is one of most widely used model systems for molecular biological studies of photosystems (Rochaix 1995; Rochaix et al. 1998) including extensive characterization of its PS II reaction center. The three dimensional model of the PS II reaction center of *C. reinhardtii*, presented here, includes D1, D2 polypeptide chains, the alpha and beta subunits of cytochrome *b559*, and the following cofactors: reaction center chlorophyll P680, four accessory chlorophylls, two pheophytins, the non-heme iron, the tetranuclear manganese cluster, two bicarbonate anions, two plastoquinones ( $Q_A$  and  $Q_B$  with modified conformations), two  $\beta$ -carotene molecules, and the heme moiety for cytochrome *b559*. The model was constructed by combining homology modeling strategy as well as incorporating the available experimental data regarding the unique features of the photosystem. We believe the availability of this almost complete model will aid in more comprehensive understanding of PS II molecular structure and the mechanism of the photochemical reactions in the PS II complex.

### Computational methods

In view of the unique nature of the current minireview in which we have discussed a newly constructed model of PS II reaction center of the eukaryotic green alga *Chlamydomonas reinhardtii*, it becomes necessary to present here, a brief discussion of the computational methods used in this work.

The homology modeling procedure for the D1/D2 proteins of the PS II reaction center of *C. reinhardtii* was carried out as described by Xiong et al. (1996) by using the QUANTA/CHARMm (version 4.1) molecular modeling program. The amino acid sequences of D1 and D2 of the green alga are according to Erickson et al. (1984) and Erickson et al. (1986), respectively. The sequence alignment of the D1 and D2 proteins with the L and M subunits of *Rb. sphaeroides* (1PCR) and *Rps. viridis* (1PRC) was primarily based on Xiong et al. (1996) with minor adjustments. The two bacterial template proteins (1PCR and 1PRC) were matched and then superimposed, and the coordinates of the aligned sequences were averaged and copied to the modeled sequences. The newly defined coordinates for D1 and D2 were briefly refined with the Structural Regularization function in QUANTA as

described earlier (Xiong et al. 1996). Certain D1 and D2 loop sequences (including the C-terminal region of D1) in between the aligned regions clearly do not exhibit homology with the L and M sequences and were treated in two different ways. For the loops of less than or equal to four residues, the conformation of the loops was built using the 'Build Coordinates' function in the Protein Design subprogram. The newly built peptide conformation was regularized as above. The sequence variable loop regions of more than four residues (including the C-terminal region of D1) were modeled using a fragment homology strategy. In this sequence-specific approach, we searched for the best matched protein sequences which have a high resolution structure, using a 'basic local alignment search tool' (BLAST, Altschul et al. 1990). The search results (not shown) produced searched fragments with high degrees of similarity to the modeled sequences; hence, the sequence homology was significant for all the searched fragments. This bits-and-pieces homology modeling strategy is based on Han and Baker (1996) and allowed us to combine the loop conformation with the rest of the modeled regions and to complete the modeling of the entire D1/D2 complex for *C. reinhardtii*.

The modeling of the N-terminal of D1/D2 was similarly directed by the alignment of D1/D2 with the bacterial L/M polypeptides. After careful refinement of the alignment in the N-terminal region, the aligned conserved residues (shown in Figure 1) were assigned coordinates from the bacterial templates. The loops were then inserted by the built-in function of QUANTA. The structure was then extensively refined by structural regularization and energy minimization procedures. The secondary structure of C-terminal residues of D1 was defined by borrowing coordinates from the BLAST-searched fragments. The modeling of the tertiary structure of the C-terminal region involves the adjustment of the location of the fragment based on the experimental suggestions that the D1 C-terminal region was involved in assembly of the Mn cluster (Britt 1996; Diner and Babcock 1996) which is in close vicinity to the donor Z (D1-Y161) and under the D1 CD helix. Since no quantitative experimental determination has been done to indicate the location of the C-terminal, there was thus a certain degree of freedom involved in our movement of the C-terminal fragments.

The PS II cofactors that have counterparts in the bacterial reaction center *Rb. sphaeroides* (1PCR) were edited using the Molecular Editor function of QUANTA and incorporated into the D1/D2 protein



Figure 1. Sequence alignment of the D1 protein of *Chlamydomonas reinhardtii* with the L subunit of the photosynthetic bacterial reaction center of *Rhodospirillum rubrum* (SL) and *Rhodospseudomonas viridis* (VL). Sequence alignment of the D2 protein of *C. reinhardtii* with the M subunit of the photosynthetic bacterial reaction center of *Rhodospirillum rubrum* (SM) and *Rhodospseudomonas viridis* (VM). The D1 and D2 sequences are in lower case and the bacterial sequences are in upper case. The secondary structure profile of the template L and M proteins and the modeled D1 and D2 proteins are also shown. The  $\alpha$ -helices are represented in cylinders. Residues that are predicted to be involved in D1/D2 interactions are marked by asterisks. Cytochrome b559 was also modeled as described in 'Computational methods'. The predicted  $\alpha$ -helices for the  $\alpha$  and  $\beta$  subunits are shown in cylinders and the predicted  $\beta$  strands are shown in arrows.

complex as described by Xiong et al. (1996). These modified structures include two chlorophylls for the special pair, two accessory chlorophylls, two pheophytins, two plastoquinones and a  $\beta$ -carotene (on the D2 side).

Further modifications were made on the conformations of certain cofactors based upon available experimental data that indicate significant variations. We modeled the two chlorophyll monomers of the chlorophyll special pair (P680) essentially according to Svensson et al. (1996), which involved a movement of the two monomers by 10 Å apart (center to center) and a rotation that allowed their  $Q_y$  excitonic transition moments to make an angle of 150°. This P680 conformation was suggested to fit all the current data (Svensson et al. 1996). The hydrogen bonding pattern of  $Q_A$  was first studied using ENDOR spectroscopy by Rigby et al. (1995). A recent study on the conformation of plastoquinone  $Q_A$  indicated that the isoprenyl chain relative to the aromatic head group is rotated by 90° at  $C\beta$  position from that in the bacterial  $Q_A$  (Zheng and Dismukes 1996). This correction was also made using the graphical interactive tools in the Molecular Editor subprogram.  $Q_B$  from the template structure of *Rb. sphaeroides* (1PCR) is not in fully bound state and is displaced by 5 Å when compared with the  $Q_B$  in the *Rps. viridis* structure (1PRC, Lancaster et al. 1995). To correct this, the position of the plastoquinone  $Q_B$  was manually moved by 5 Å to match the superimposed  $Q_B$  of the 1PRC structure. Two bicarbonate anions were also docked into the model at the non-heme iron and the  $Q_B$  sites, as described by Xiong et al. (1996). Based on EPR and site-directed mutagenesis experiments (Koulougliotis et al. 1994; Hutchison and Sayre 1995), there are two extra accessory chlorophylls that may be liganded to residues D1-H118 and D2-H117. They were included by manually docking them into these sites. An additional  $\beta$ -carotene molecule suggested to exist on the D1 side of the PS II reaction center was modeled in the symmetrical position (relative to the central axis of the reaction center) of the  $\beta$ -carotene on the D2 side, which is a homologue of the bacterial carotenoid. (For roles of carotenes in PS II reaction centers, see Trebst and Depka 1997; and Depka et al. 1998.)

The D1/D2 protein structure combined with the above cofactors was energy-minimized using the CHARMM protocols (Brooks et al. 1983). The energy minimization was performed until convergence was reached (rms force < 0.01 kcal/mol·Å<sup>2</sup>), as described by Xiong et al. (1996). During this process, the coordinates of all the cofactors were constrained in place

and only the D1 and D2 polypeptides were allowed to move.

After the energy minimization of the protein/cofactor complex, a tetramanganese cluster along with Ca and Cl was added into the D1/D2 model. The Mn cluster was modeled separately as an open, C-shaped structure as suggested by Klein et al. (1993) and Dau et al. (1995). Other necessary details will be provided later in the paper. Following the addition of the Mn cluster energy minimization (500 ABNR iterations) of the C-terminal region was performed.

Cytochrome *b559*, an intrinsic transmembrane protein of the PS II reaction center (Cramer et al. 1993; Whitmarsh and Pakrasi 1996), has no homologous bacterial templates to aid the homology modeling. This protein, having two subunits,  $\alpha$  and  $\beta$ , was modeled exclusively based on existing information in literature, as discussed in the text of this minireview. Transmembrane  $\alpha$ -helices of the  $\alpha$  (residues 18–43) and of the  $\beta$  (residues 18–43) subunits were assigned according to Cramer et al. (1993) and Whitmarsh and Pakrasi (1996) and the cytochrome was modeled in the  $\alpha/\beta$  heterodimer form. The conformations of the N- and C-terminal regions of the  $\alpha$  subunit and the N-terminal region for the  $\beta$  subunit were modeled using the BLAST approach, as mentioned above. The newly modeled terminal regions were combined with the helical regions and refined by energy minimization. The  $\alpha$  and  $\beta$  polypeptide chains were then combined with a heme group, allowing the histidine residue from each subunit ( $\alpha$ -H23 and  $\beta$ -H23) to form a ligand to the heme iron. The structure of the heme moiety was obtained from that of cytochrome *b562* of *Escherichia coli* (PDB file code, 256B). The  $\alpha$  and  $\beta$  subunits together with the heme were docked in the D1/D2 complex on the  $Q_B$  side with the  $\beta$  subunit in close association with helix E of the D1 protein. The docking of cytochrome *b559* also took consideration of the following experimental information: the estimated distances of the heme iron to  $Q_B$  (C2) and P680 (Mg) are 20 and 35 Å, respectively (Shuvalov 1994); and, the N terminus of the  $\alpha$  subunit is cross-linked to the D1 DE loop region (D1-F239 to D1-E244) (Barbato et al. 1995). The contact region of the combined D1/D2/cytochrome *b559* was further minimized to obtain the finalized model (500 ABNR iterations).

In summary, the modeling of the *C. reinhardtii* D1/D2 proteins was based on homology with the L/M subunits of both *Rps. viridis* and *Rb. sphaeroides*. The D1 and D2 proteins were aligned with the L and M subunits, respectively. The alignment was primarily based on the modeling of the PS II reaction center

of *Synechocystis* 6803 (Xiong et al. 1996) with minor adjustments (Figure 1). After alignment, we find 27% sequence identity (92 residues) and 56% sequence similarity (194 residues) for D1 with the L subunit and 24% sequence identity (83 residues) and 63% sequence similarity (217 residues) for D2 with the M subunit.

The entire modeling work was performed on UNIX Silicon Graphics Power Series Workstation 4D/440VGXT. Copies of the coordinates of this model in PDB format are available on request from the authors.

### Description of the *Chlamydomonas* PS II model

As expected and is well known (Trebst 1986), the general topology of the D1/D2 model resembles that of the L/M structure of the bacterial reaction center, each containing five transmembrane  $\alpha$ -helices (Figures 1 and 2A) denoted as A, B, C, D and E. There are also several short non-membrane  $\alpha$ -helices between the transmembrane helices on both the luminal and stromal sides, which are denoted as CD, DE, etc. The detailed secondary structure profiles analyzed from the modeled D1, D2 and cytochrome *b559* are also shown in Figure 1. The definition for the boundaries of the transmembrane  $\alpha$ -helices (cylinders in Figure 1) are slightly different from those in earlier PS II models (Ruffle et al. 1992; Svensson et al. 1996; Xiong et al. 1996). The interface between D1 and D2 was also examined which is mostly composed of residues in the N-terminal and C-terminal regions of D1 and D2, as well as the transmembrane helices D and E (marked under the sequences in Figure 1). The contact residues are thought to provide the key protein-protein interactions maintaining the proper conformation of the reaction center complex. Further, certain contact sites between D1 and D2 have been proposed to be especially susceptible to proteolytic cleavage in the rapid turnover of the D1 protein during exposure to high light (Trebst 1991; Trebst and Soll-Bracht 1996).

In the current PS II reaction center model, the modeled cofactors bound to D1/D2 include six chlorophylls, two pheophytins, two  $\beta$ -carotenes, two plastoquinones, a tetramanganese cluster with calcium and

chloride liganded, one non-heme iron and two bicarbonate ions (Figure 2A). The structures of most of the cofactors are arranged in a two fold symmetry relative to the central axis of the reaction center. It is important to note here that the prosthetic groups in the *Synechocystis* sp. PCC 6803 model (Xiong et al. 1996) did not have idealized geometry owing to distortions arising from unconstrained energy minimization. However, the current *Chlamydomonas* model has idealized geometry for the prosthetic groups. The stoichiometry and geometry of the above cofactors modeled is consistent with the consensus of the published experimental data (Nanba and Satoh 1987; Gounaris et al. 1990; Kobayashi et al. 1990; van Leeuwen et al. 1991; Chang et al. 1994; Eijkelhoff and Dekker 1995; Pueyo et al. 1995; Zhelva et al. 1996). The combined protein and cofactor model of the *C. reinhardtii* PS II reaction center is shown in Figure 2B. We will describe below mainly the features of the newly modified or added cofactors beyond what has been published recently (Svensson et al. 1996; Xiong et al. 1996). Table 1 provides the names and the numbering of the amino acids that form the binding niches of the various cofactors discussed below.

### Chlorophylls

In a previous *Synechocystis* PCC 6803 model with D1/D2 and cofactors (Xiong et al. 1996), various possible conformations of P680 were discussed. It was concluded that the P680 conformation for which the special pair is perpendicular to the membrane was the preferred conformation. In this current model, that has idealized geometry of the prosthetic groups, the two monomers of the P680 chlorophyll dimer were further modified according to Svensson et al. (1996) to allow the center-center distance of the two monomers to be 10.0 Å and their  $Q_y$  excitonic transition moments to be at an angle of 150° (Figures 3 and 4). (This is different from the arrangement of the two bacteriochlorophylls in the 'special pair' of the bacterial reaction center.) Such P680 conformation was suggested to match all existing experimental data on the primary donor (Svensson et al. 1996). Those magnesium ions at the center of the two chlorophyll monomers are liganded by two specific histidine residues, D1-H198 and

Figure 2. (A) The modeled cofactors in the PS II reaction center (see 'Computational methods') shown in liquorice bond forms. (B). The combination of D1/D2/cytochrome *b559* proteins and the bound cofactors. The ribbon form indicates the  $\alpha$ -helices. D1 and D2 all have five transmembrane helices and several amphipathic helices in the luminal (bottom) and stromal (top) sides. Cytochrome *b559* was modeled in  $\alpha/\beta$  form; each subunit has one transmembrane helix.

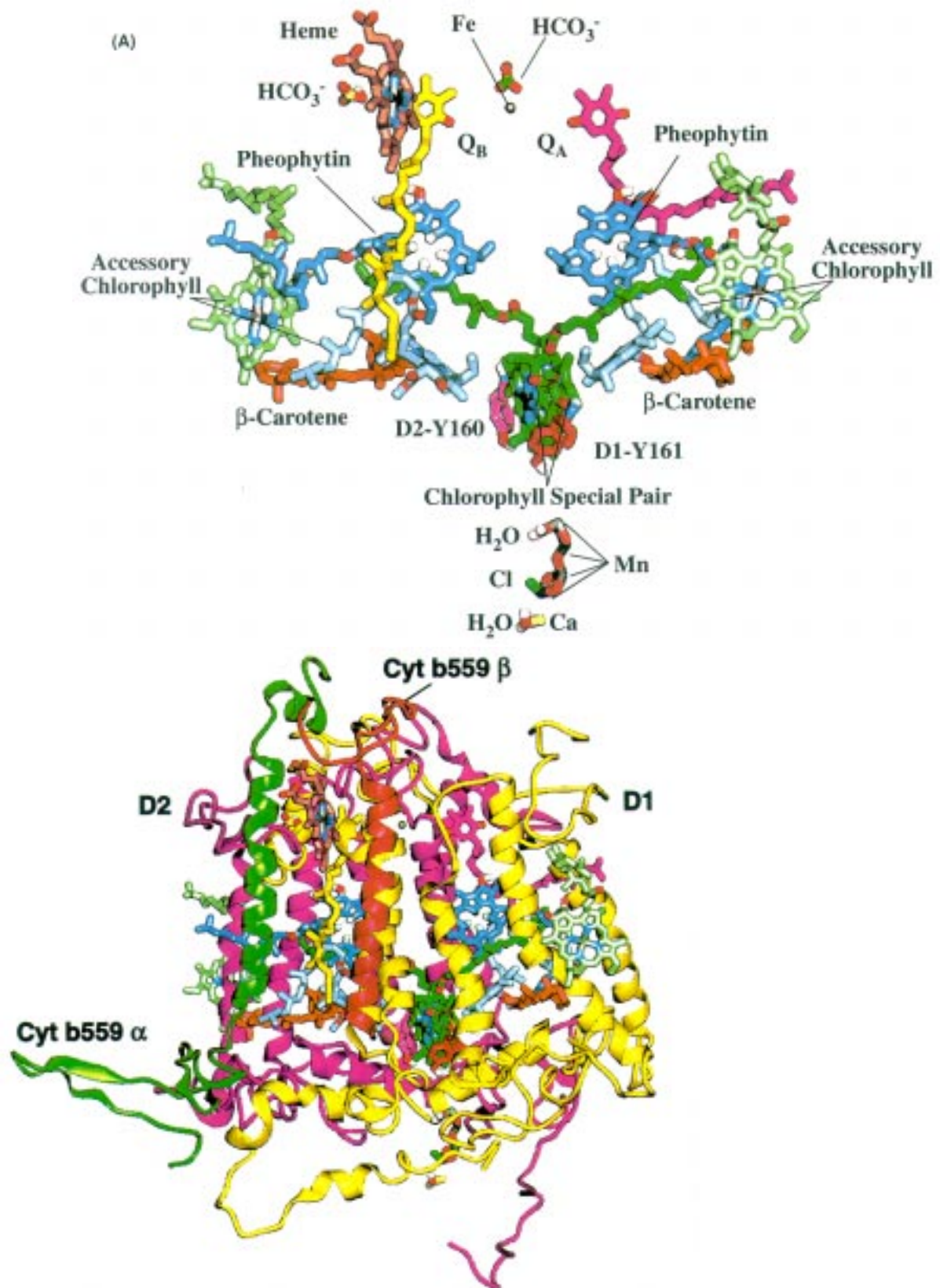


Figure 2.

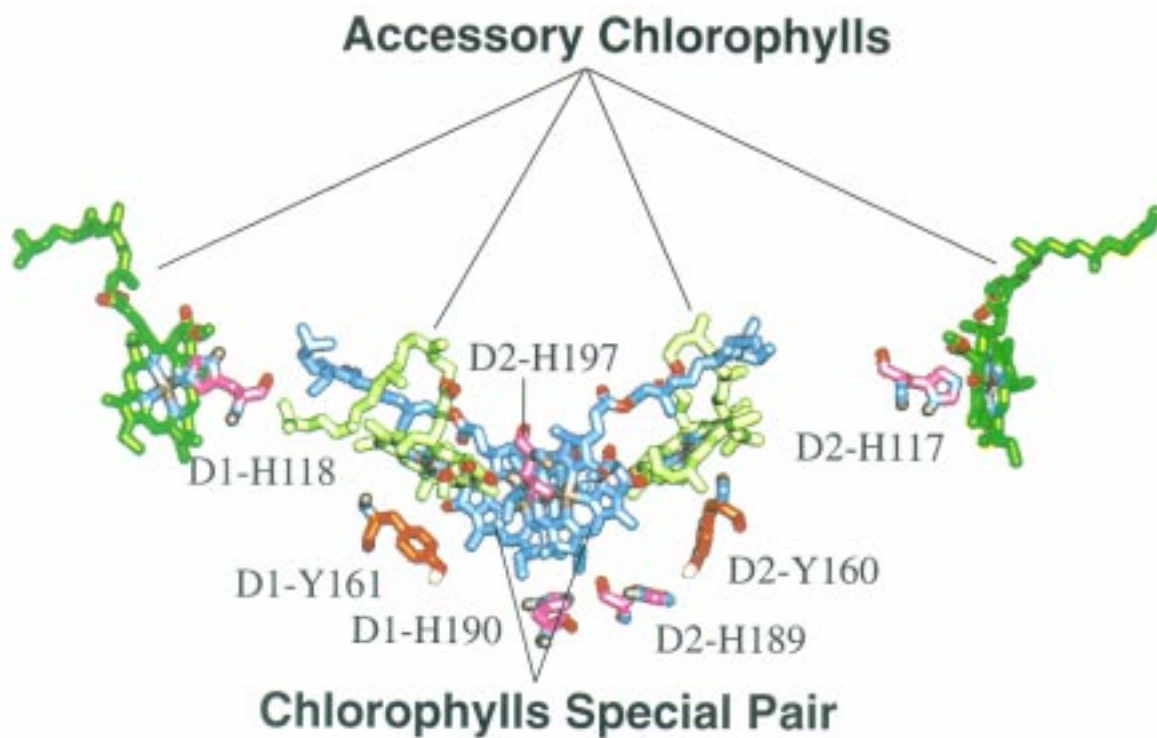


Figure 3.

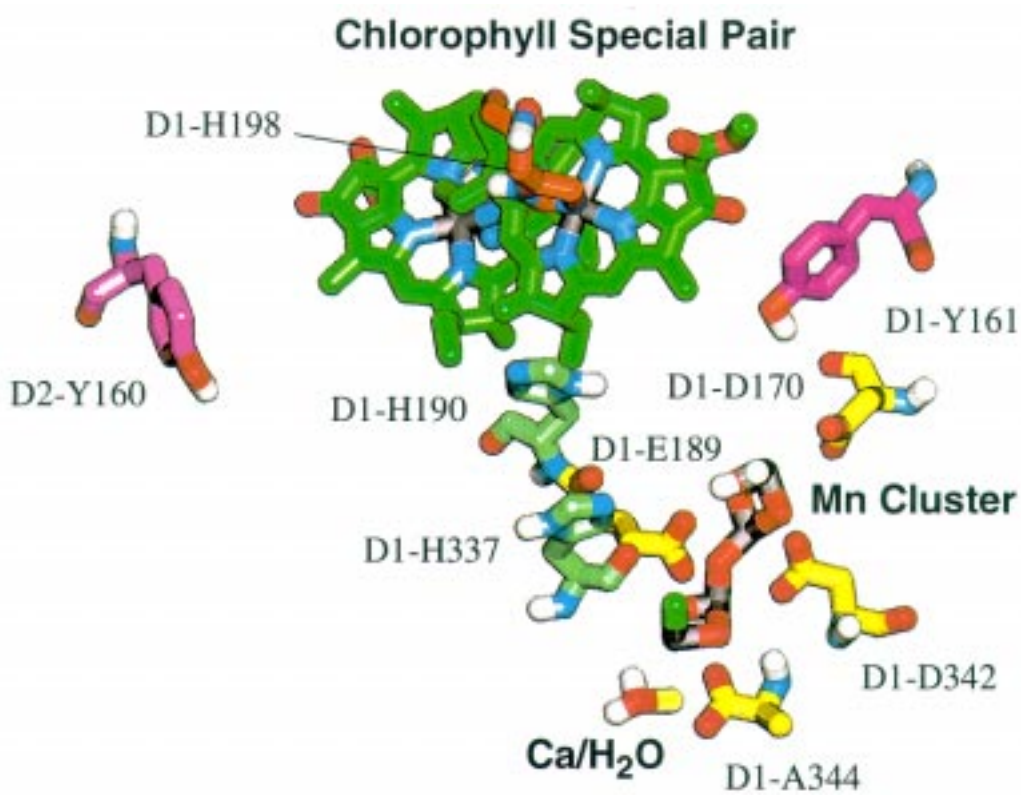


Figure 4.

D2-H197, which, according to sequence comparison, match well with L-H173 and M-H210 (*Rps. viridis* numbering) of the bacterial special pair ligands (Figures 3 and 4). Mutations at these two histidine residues have strongly implicated the role of the two residues in coordinating the P680 (Vermaas et al. 1988; Nixon et al. 1992).

Based on out-of-phase ESEEM (electron spin echo envelope modulation measurements), the distance from P680 to Q<sub>A</sub> has been evaluated to be  $27.4 \pm 0.3$  Å in samples lacking non-heme iron (Zech et al. 1997). Hara et al. (1997) have confirmed, also by ESEEM spectroscopy, the same distance to be  $27.2 \pm 1.0$  Å in three different PS II preparations. Our model predicts this distance to be within one Å of those reported in the literature.

In our current model, two of the accessory chlorophylls were modeled based on their counterparts in anoxygenic bacteria (Figure 3). We further note that the fifth and the sixth chlorophylls (the accessory chlorophylls here) of the D1 and the D2 are also equivalent to the cC and cC' chlorophylls of the PSI (Krauss et al. 1996). As in previous models (Ruffle et al. 1992; Xiong et al. 1996), these two chlorophylls have no conserved histidine ligands in D1 and D2. Svensson et al. (1996) had proposed a possibility that water molecules may act as ligands for the chlorophylls. This possibility may be considered analogous to that in the crystal structure of peridinin-chlorophyll-protein of *Amphidinium carterae* (Hofmann et al. 1996) which shows a chlorophyll liganded by a water molecule.

Several experiments have indicated that two additional accessory chlorophylls may exist and may be liganded by D1-H118 and D2-H117 (D2-H118 in plants) (Koulougliotis et al. 1994; Hutchison and Sayre 1995; Mulkidjanian et al. 1996). We have, thus, included two such accessory chlorophylls (termed chlorophyll<sub>z</sub>s) perpendicular to the membrane and allowed them to be liganded by the above two histidines (Figure 3). In this model, the two chlorophyll<sub>z</sub>s mod-

eled to D1-H118 and D2-H117 are separated from the non-heme iron by 36.1 Å and 40.4 Å (from Mg to Fe), respectively, which matches the experimentally determined value of  $39.5 \pm 2.5$  Å (Koulougliotis et al. 1994). The center-to-center distances of the two accessory chlorophylls to P680 are 30.4 Å and 32.3 Å, for the D1 and D2 chlorophyll<sub>z</sub>s, respectively, which also match the experimental determination of 30 Å (Schelvis et al. 1994). The distance from the magnesium of D1-chlorophyll<sub>z</sub> to the magnesium of other accessory Chl of D1 is 23 Å, whereas the distance from it to the magnesium of the Chl of P680 on the D1 side is 10.8 Å. On the other hand, similar distances on the D2 side are 24.9 and 12.5 Å, respectively. Although there is a symmetry in the molecule, the above distances suggest that the symmetry is not perfect, and this may be one of the factors, no matter how small, in predicting widely different rates of electron flow on the two sides of the molecule. It may also be useful in interpreting the heterogeneous charge separation data, related to equilibration of excitation energy amongst the different Chl and pheophytin molecules in PS II reaction centers (Greenfield et al. 1997). Site-directed mutagenesis on D1-H118 in *C. reinhardtii* also indicates the strong possibility of D1-H118 to be a chlorophyll liganding residue (Hutchison and Sayre 1995). A modelling result of the chlorophyll<sub>z</sub>s was first presented in a review by Nugent (1996).

As shown in Figures 2A and 2B, the two chlorophyll<sub>z</sub> molecules are actually located towards the exterior of the D1/D2 complex and their binding may involve other PS II core proteins. It is conceivable that in some PS II reaction center preparations, these two chlorophylls may be easily lost when preparing the PS II reaction center resulting in occasionally different number of chlorophylls per reaction center (ranging from 4 to 6) and hence the controversies in experimental determinations (Nanba and Satoh 1987; Barber et al. 1987; Gounaris et al. 1990; Kobayashi et al. 1990; van Leeuwen et al. 1991; Moskalenko et al.

---

←  
 Figure 3. The modeled conformation of six chlorophylls in the *C. reinhardtii* PS II reaction center. The center of the chlorophyll special pair (P680) is coordinated by two histidines (D1-H198 and D2-H197). Two accessory chlorophylls on the exterior of the reaction center are liganded by another two histidines (D1-H118 and D2-H117). Two redox active residues D1-Y161 (Z) and D2-Y160 (D) as electron donors to P680 are also shown. D2-H189 is also shown as interacting with D2-Y160 through hydrogen bonding. D1-H190 is thought to be homologous to D2-H189 but is not modeled within the hydrogen bonding distance to D1-Y161.

Figure 4. The model for tetramanganese cluster. The conformation of the Mn cluster is according to Klein et al. (1993) and Dau et al. (1995). The calcium and chloride anions were modeled according to Babcock (1995). The putative amino acid ligands to the Mn are also shown. The relative position of the cluster with the donors Z and D and P680 chlorophylls are also shown. For clarity, the phytol groups of the chlorophyll special pair were not shown.

1992; Chang et al. 1994; Eijkelhoff and Dekker 1995; Pueyo et al. 1995, Zheleva et al. 1996; Eijkelhoff et al. 1997; Kurreck et al. 1997).

### *$\beta$ -Carotenes*

Carotenoids in the PS II reaction center are suggested to function in protecting this complex against photo-oxidation by quenching the triplet state of the primary electron donor P680 (Frank and Cogdell 1996) although the triplet of carotene has not been established to be an intermediate. In isolated PS II reaction center preparations, the majority of the reports indicate that there are two carotene molecules per PS II reaction center (Gounaris et al. 1990; Kobayashi et al. 1990; Montoya et al. 1991; De Las Rivas 1993; Eijkelhoff and Dekker 1994; Mimuro et al. 1995). Further, it has been suggested that the two carotenes may be excitonically coupled (Kwa et al. 1992). We have modeled two  $\beta$ -carotene molecules in the D1/D2 protein complex, one which is located on the D2 side was modeled by modifying the structure of dihydro-neurosporene from *Rb. sphaeroides* (1PCR), and the other by docking a  $\beta$ -carotene on the D1 side (see Trebst and Depka (1997); and Trebst et al. (1998) for a discussion of the role of carotenes in PS II reaction centers). As a first approximation, this conformation is consistent with the idea of symmetry of the reaction center: the D1  $\beta$ -carotene is docked in a symmetrical position, relative to the central axis of the reaction center, to that of the D2  $\beta$ -carotene. There are controversies regarding the orientation of the one carotene with respect to the other, as well as regarding the configuration of  $\beta$ -carotene in the PS II reaction center. Clearly, the model is speculative and needs to be tested. Earlier data (Fujiwara et al. 1987) had suggested that the  $\beta$ -carotene adopts a *trans* configuration. However, recent data (Bialek-Bylka et al. 1995), obtained by extracting carotenoids in complete darkness, indicate that the carotenoids in the PS II reaction center adopt a 15-*cis* configuration consistent with the central mono-*cis* structure as observed for the carotenoids in all bacterial reaction centers. We consider this work more reliable than the older work and, thus, in our modeling we used the *cis* configuration for the carotenoids. In fact, the  $\beta$ -carotene found in the PSI reaction center also has a 15-*cis* configuration (Bialek-Bylka et al. 1996). The universal *cis* configuration of  $\beta$ -carotene in all photosynthetic reaction centers contrasts with all *trans*-configuration found in the light harvesting complexes (Frank and Cogdell 1996). Thus, this particular natural selection for the *cis* configuration in the reaction center

appears to have some advantages over the other configuration in performing the photo-protective function. However, the answer to the question of orientation of one carotene with respect to the other would have to wait for further modeling and experiments.

In this modeling, each carotenoid was modeled to be within the van der Waals contact distance with two accessory chlorophylls, one 'proximal' accessory chlorophyll close to the special pair, and the other 'distal' accessory chlorophyll liganding to D1-H118 or D2-H117. The close proximity of  $\beta$ -carotene to the accessory chlorophyll suggests a high probability of its function in quenching the triplet state of primary donor P680 via the accessory chlorophyll, analogous to the role of the carotenoid in the reaction center of anoxygenic bacteria. However, no positive data are available on this point. In light of the insufficient information on the location of the  $\beta$ -carotene molecules, we consider the docking of the  $\beta$ -carotenes on the reaction center protein highly tentative, but challenging. However, the model provides information on the nearest neighbor amino acid residues that can be tested through site-directed mutagenesis (see Table 1).

### *Donors to the oxidized form of reaction center chlorophyll pair P680: The tyrosines*

Also shown in Figure 3 are two tyrosine residues, D1-Y161 and D2-Y160, which are electron donors to the oxidized form of the reaction center chlorophyll P680 (known as the donors Z and D, or  $Y_Z$  and  $Y_D$ ). Their roles as donors to  $P680^+$  were clearly demonstrated by site-directed mutagenesis studies (Vermaas et al. 1993; Britt 1996). The two tyrosine residues, both with their hydroxyl groups pointing toward the lumen, are arranged symmetrically around the special pair chlorophylls. The modeled distance from the D1-Y161 phenolic oxygen to the magnesium of the nearest chlorophyll of the P680 dimer is 12.5 Å, which matches with the experimentally determined distance of 10–15 Å (Hoganson and Babcock 1989); however, the distance from the same hydroxyl oxygen to the oxygen of the carbonyl group (on the 5th ring) of the same Chl is only 8.5 Å. The measured distance between the phenolic oxygens of D1-Y161 and D2-Y160 are 31.3 Å which matches with the experimentally measured 29–30 Å distance in spinach (Astashkin et al. 1994; Kodera et al. 1995). The modeled distances of the phenolic oxygens of tyrosines Z and D to the non-heme iron are 37.4 Å and 37.1 Å, respectively, which fall in the range of the EPR spectroscopic measurements of  $37 \pm 5$  Å by Koulougliotis et al. (1995)

using *Synechocystis* PS II core preparations. Out-of-phase ESSEM measurements on iron-depleted PS II have suggested that the distance from oxidized D1-Y161 to  $Q_A$  must be  $> 32 \text{ \AA}$  (Zech et al. 1997); distance measurements, based on our model, are: from hydroxyl oxygen of D1-Y161 to C6 of  $Q_A$ ,  $35.3 \text{ \AA}$ ; from alpha C of the tyrosine to C6 of  $Q_A$ ,  $33.1 \text{ \AA}$ . Further, the distances to C6 of  $Q_A$  from the alpha C and the hydroxyl oxygen of D2-Y-160 are  $36.5$  and  $37.8 \text{ \AA}$ , respectively. The above experimental studies provide strong support to the validity of the current PS II three-dimensional model, presented here.

In our model, the distance from the phenoxy oxygen of D1 tyrosine-161 to the C4 phenol of Phe-186 is  $6.2 \text{ \AA}$ ; and to the closest oxygen of carboxyl of Asp-170, it is  $5.6 \text{ \AA}$ . Further, the distance from the backbone C of Gln-165 to the carboxyl oxygen of tyrosine-161 is  $5.4 \text{ \AA}$ . Most of these distances are much larger (by almost  $1\text{--}2 \text{ \AA}$ ) than those modeled by Kless and Vermaas (1996), by another method, for the wild-type *Synechocystis* sp. PCC 6803. It is worth mentioning that these authors explicitly stated that they only rely on the differences they observed between the wild type and the mutants they had constructed. However, even this needs further investigation.

The donor D (D2-Y160) is modeled at a close distance to a histidine residue D2-189: the distance from the oxygen of the hydroxyl of tyrosine to  $\epsilon 2$ -nitrogen of histidine is  $4.0 \text{ \AA}$  ( $3.1 \text{ \AA}$ , from the hydroxy hydrogen of D2-Y160 to  $\epsilon 2$ -nitrogen of D2-H189) which allows for weak hydrogen bonding interactions. Further, we note that the distance from the same hydrogen to  $\delta 1$  nitrogen of the same histidine is a bit larger,  $4.4 \text{ \AA}$ . Spectroscopic studies on the site-directed mutants of D2-H189 in *Synechocystis* 6803 strongly supports its proposed interaction with the donor D (Tang et al. 1993; Tommos et al. 1993). It was suggested that D2-H189 may function to accept the proton from D2-Y160 upon oxidation of D (Svensson et al. 1996). The ESE-ENDOR experiment of Campbell et al. (1997) has shown that D2-H189 is a direct ligand to D2-Y160 with its  $\tau$  nitrogen pointed toward  $Y_D$ , consistent with our current model. This close interaction was, however, not observed in our previous model (Xiong et al. 1996); we attribute this inconsistency to the slightly different methodology used during the modeling processes. However, we consider the current model an improved version of the earlier model.

In the D1 protein, the residue homologous to D2-H189 is D1-H190. The distance from the oxygen of the hydroxyl in tyrosine to  $\delta 1$ -nitrogen of histidine is  $9.0 \text{ \AA}$ , and  $10.8 \text{ \AA}$  to its  $\epsilon 2$ -nitrogen. We also note that

the hydrogen of NH in D1-H190 is  $8.2 \text{ \AA}$  away from the hydroxy oxygen of the donor Z, the D1-tyrosine-161; the distance from the closest ring N of His-190 is  $8.9 \text{ \AA}$ . Kless and Hadar (1996) had modeled it to be  $6.1 \text{ \AA}$ , whereas Svensson et al. (1996) had this distance to be  $4 \text{ \AA}$ . Ruffle et al. (1992) had modeled the histidine beyond hydrogen bonding distance from  $Y_Z$ . Thus, a geometric homology between the two histidine residues does not appear to exist. Mutation of D1-H190 residue to a phenylalanine gives spectroscopic data similar to the wild type, supporting the suggestion that the histidine may not be in close contact with the donor Z (Kramer et al. 1994; Roffey et al. 1994); this is inconsistent with the conclusion of Svensson et al. (1996) who have proposed a possible electrostatic interaction between the two residues. On the other hand, this histidine residue is believed to be involved in the assembly of the manganese cluster, and its closest distance (from  $\delta 1$ -hydrogen of the side chain of histidine to one of the hydrogens (H1) of the water molecule liganded to the Mn cluster) was modeled to be  $7.0 \text{ \AA}$  (see below). Further, we note that if this measurement was made to individual Mn atoms, it would be still farther ranging from  $8.9$  to  $11.5 \text{ \AA}$ .

#### *Tetramanganese cluster*

The presence of Mn on the luminal side of the PS II reaction center was first indicated by Fowler and Kok (1974) from their proton release experiments, whereas Blankenship and Sauer (1974) showed that Mn was released into the lumen upon Tris treatment and explicitly proposed that Mn resides on the luminal side of the membrane. Further, Coleman and Govindjee (1987) were the first to propose that Mn atoms were bound to specific amino acids on the luminal side of the D1/D2 proteins. Since then extensive biochemical and molecular biological studies have been made in analyzing the structure and function of manganese ions in the involvement of water oxidation. A previous attempt to model Mn cluster in the D1/D2 protein model was that by Ruffle and Nugent (1992). In the present study, we have modeled the tetramanganese cluster along with calcium and chloride within the PS II reaction center. The tetramanganese cluster, which is located within the PS II reaction center, mediates the oxidation of water to form molecular oxygen. During this process, electrons are extracted to reduce the oxidized donor Z (Britt 1996; Yachandra et al. 1996). Extensive biochemical and spectroscopic studies have given significant new insights into the structure of this tetramanganese cluster. Several structural models for

the Mn cluster, based on extensive experimental results, are available (Klein et al. 1993; Dau et al. 1995; Babcock 1995). After evaluating the various models of the Mn cluster, we chose the model of M. Klein, V. Yachandra and co-workers, remodeled the Mn cluster along with Ca and Cl, and then incorporated it into our constructed PS II reaction center protein model. The Mn cluster was first modeled separately as an open, C-shaped structure as suggested by Klein et al. (1993) and Dau et al. (1995). For convenience, all four Mn ions in this model were modeled in the +3 state, which were linked together by mono- or di- $\mu$ -oxo bridges. The distances of Mn-Mn were modeled to be 2.7 Å for the two oxo species and 3.3 Å for the single oxo species as indicated by the X-ray absorption spectroscopy studies (Dau et al. 1995). The set of angles between the Mn-Mn vector (a imaginary line between two Mn atoms) relative to the membrane normal (a vertical axis running across the membrane) was modeled to be 68°, 30° and 57°, respectively. The first and the third angles are for the two di- $\mu$ -oxo bridges and the second is for the mono-oxo bridge. A calcium ion (Ca<sup>2+</sup>) and a chloride ion (Cl<sup>-</sup>) which are also essential for water oxidation were appended to the tetramanganese center, the modeling of which was according to Babcock (1995). The chloride was modeled to ligand to one of the Mn on the open end of the C-shaped structure. A substrate water molecule was modeled to bind to a terminal Mn and another water was modeled to bind to the calcium on the opposite end of the cluster.

In the models of Coleman and Govindjee (1987) and Padhye et al. (1986) and Babcock (1995), amino acids with carboxylic groups as well as a histidine residue are ligands to the Mn/Ca ions. Site-directed mutagenesis studies on both D1 and D2 have suggested a number of candidates as Mn liganding residues (Debus 1992; Britt 1996). Among them, D1-D170 was suggested to be a key ligand during photoactivation of oxygen evolution machinery while assembling the Mn cluster (Nixon and Diner 1992), even though this residue appears not to be involved in the steady state turnover. Thus, in our tentative modeling of the Mn cluster, this residue served as a target in our initial docking. Its orientation was then further manipulated to allow it to be in close vicinity of other carboxylic groups or histidine residues, as described by Klein et al. (1993) and Dau et al. (1995). During this process, the side chains of the relevant amino acid residues with carboxylic groups on the D1 C-terminus were also moved such that they became closer to D1-D170 and the Mn cluster.

Potential carboxylate ligands to the Mn cluster have been suggested to be D1-D170, D1-E333, D1-D342 and D1-A344 (Coleman and Govindjee 1987; Babcock 1995). Whereas three of the above residues appear to fall into the Mn binding domain (a 5 Å sphere that allows van der Waals interactions), D1-E333 is located too far from the putative Mn binding domain to be considered as a likely binding residue. However, D1-E189 was in close vicinity to the carboxylate ligands to provide a pair of carboxylate bridges to the Mn cluster (Figure 4). Histidine residues D1-H190, D1-H332 and D1-H337 were suggested to be the potential cluster ligands (Babcock 1995). We consider D1-H337 a more likely ligand than the other two due to the closer spatial proximity. The direct involvement of D1-H337 in Mn binding was strongly supported by site-directed mutagenesis and EPR analysis (Bowlby et al. 1996). D1-H190, in conjunction with D1-E189, was proposed to be involved in a proton shuffling pathway extracting protons from the water oxidation complex (Babcock 1995) and is also shown in Figure 4. Amino acid residues found within the van der Waals distance (5 Å), or at slightly larger distance, from the Mn cluster, which appear to form the Mn binding pocket, are D1-L91, D1-D170, D1-F182, D1-E189, D1-H190, D1-M293, D1-N296, D1-N301, D1-A336, D1-H337, D1-N338, D1-F339, D1-P340, D1-L341, D1-D342, D1-L343 and D1-A344. Among them, residues D1-F182, D1-F339, D1-L341 and D1-L343 are non-polar and are not likely to provide strong direct interactions to the Mn cluster. A histidine residue, D1-H332, is not included in the 5 Å sphere (the  $\delta$ 1 nitrogen of the histidine is 12.5 Å away from the calcium ion), but it may be somehow important for the assembly of the Mn/Ca cluster. Further, we note that distances from  $\delta$ 1 nitrogen of histidine to the individual Mn atoms range from 13.7 to 20.2 Å, and those from  $\epsilon$ 2-nitrogen of histidine to individual Mn atoms to range from 15.6 to 22.3 Å. Site-directed mutagenesis on D1-H332 as well as D1-E333, D1-H337, and D1-D342 indicates that they may influence the assembly and/or stability of the Mn cluster (Chu et al. 1995).

In the current model, the 'center to center' distance between D1-Y161 and the Mn cluster is 14.5 Å (from  $\gamma$ -carbon of D1-Y161 to the 'central' oxygen of the Mn cluster), which could be consistent with the most of the experimental data known to date. We note that if one measures the distance from the oxygen of the hydroxyl group of this tyrosine to the individual oxygens of the Mn cluster, it ranges from 8.0 to 13.6 Å, whereas that to individual Mn atoms, it ranges from

6.9 to 14.1 Å. Noguchi et al. (1997) have recently provided evidence, using Fourier Transform Infrared Spectroscopy, that a Mn cluster and a tyrosine is linked via a chemical and/or hydrogen bonds and that structural changes of the Mn cluster are transmitted to the tyrosine through these bonds. If this is proven to be true, then a tyrosine, other than D1-Y-161, may have to be considered, or, a mechanism must be sought to explain the apparent contradiction. However, the distance, in our model, from the hydroxyl oxygen of D2-Y160, to various oxygens of the Mn cluster ranges from 29.5 to 32.0 Å, much farther than from D1-Y161. Thus, the D2-Y160 cannot be the tyrosine studied by Noguchi and co-workers. This further emphasizes the asymmetry of the two sides and reasons for the differences between D1-Y-161 and D2-Y-160. A difference in accessibility of the two tyrosines to outside agents was recently published by Li et al. (1997). The distance of about 15 Å between Y<sub>Z</sub> and the Mn cluster is supported by the following observations: (1) analysis of electrochromic absorption changes (Mulikidjanian et al. 1996); (2) spin lattice relaxation measurements of Kodera et al. (1995); (3) high field EPR analysis of Un et al. (1994); and (4) kinetic measurements of 355 nm absorption changes at different temperatures (Karge et al. 1997). However, this distance between the two redox groups is still a matter of debate. The ESE-ENDOR spectroscopic experiments of Gilchrist et al. (1995) showed a close proximity (4.5 Å) between the Mn cluster and Y<sub>Z</sub>. On the other hand, the pulsed EPR study of Astashkin et al. (1997) questions the interpretation of 4.5 Å value in reflecting the distance between Y<sub>Z</sub> and the Mn cluster. We modeled the Mn cluster after considering the above distance constraints as well as the components of its coordination sphere which is mainly composed of carboxylate residues. Furthermore, the modeled distance between the Mn and donor Y<sub>D</sub> is 30.2 Å (from the central oxygen of the Mn cluster to the ζ-carbon of D2-160), and ranges from 29.5 to 30.2 Å even when the distance is measured to the individual Mn atoms. (The distance from ζ carbon of the D2-Y-160 to the various oxygens of the Mn cluster range from 29.5 to 32.0 Å, and from hydroxyl oxygen to the oxygens of the Mn cluster to range from 28.3 to 30.9 Å.) These data agree with the 28–30 Å value of distance between D2-Y-160 and the Mn cluster, as determined by a pulsed EPR selective hole burning experiment (Kodera et al. 1994); and 30 ± 0.2 Å by ESE-ENDOR method (Hara et al. 1996).

Research on the mechanism of charge and proton transfer in the water oxidation complex has led to the proposal of a redox cofactor X in the water oxidation

complex accepting protons during the S-state transition (Haumann et al. 1996, 1997a, b; Hundelt et al. 1997). X has been tentatively assigned to be a histidine residue. This assignment is consistent with the earlier data of Allakhverdiev et al. (1992) and Berthomieu and Boussac (1995). If we consider this assignment valid, the histidine can be either D1-H190 (see above) or D1-H337 due to their close proximity. The distance from the δ1-hydrogen of D1-H190 to the H1 of the water molecule liganded to the Mn cluster is 7.0 Å, but from the δ2-carbon to the chloride liganded on the Mn cluster, it ranges from 9.8 to 11.2 Å as there are several carbon atoms. We note, however, that distances from ε1-nitrogen of histidine to individual Mn atoms range from 8.9 to 10.1 Å; and from δ1 nitrogen to individual Mn atoms, the distance ranges from 8.9 to 11.5 Å. Bögershausen et al. (1996) proposed that the oxidized form of Y<sub>Z</sub> is stabilized by a nearby base 'B'. We, however, did not find any basic residues within a 5 Å distance from D1-Y161 in our current model. The nearest basic residues are D1-H190 and D1-H195 which are modeled to be in a range of 8.0 to 10.8 Å from the donor Z (8.2 and 9.8 Å, from hydroxy-oxygen of D1-Y160 to δ1-hydrogens of NH group of D1-H190 and D1-H195, respectively; distances from the hydroxy oxygen of the tyrosine to δ1-nitrogen and to ε2-nitrogen of D1-H190 are 9.0 and 10.8 Å, respectively). If such a 'base' indeed exists near Y<sub>Z</sub>, we are unable to provide any information on it from our model. We cannot rule out the possibility that a remote base functions in a manner that we do not yet know and understand.

#### *Cytochrome b559 and the heme binding region*

Cytochrome *b559* is an intrinsic and essential component of the PS II reaction center (Cramer et al. 1993; Whitmarsh and Pakrasi 1996). Its presence is critical for the biogenesis and stable assembly of the PS II reaction center. Though this protein is not involved in the primary electron transport in PS II, experimental studies suggest that it may be involved in protecting PS II from photodamage in excess light. However, since this protein is absent in anoxygenic photosynthetic bacteria, it has no available homologue for direct modeling. Thus, it presents a challenge to modeling the structure *de novo* not only at the secondary and tertiary levels, but also at the quaternary level. In this work, knowledge on the experimental characterization of this protein is exclusively employed for constructing the model. The relevant literature is briefly summarized below.

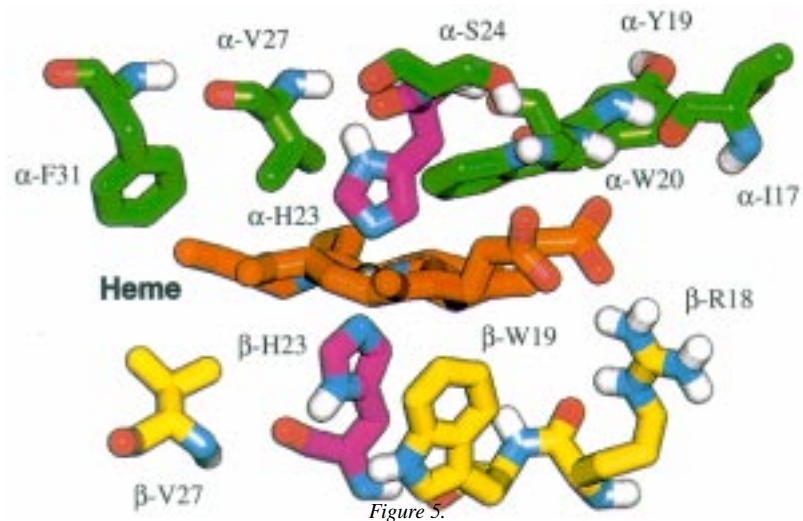


Figure 5.

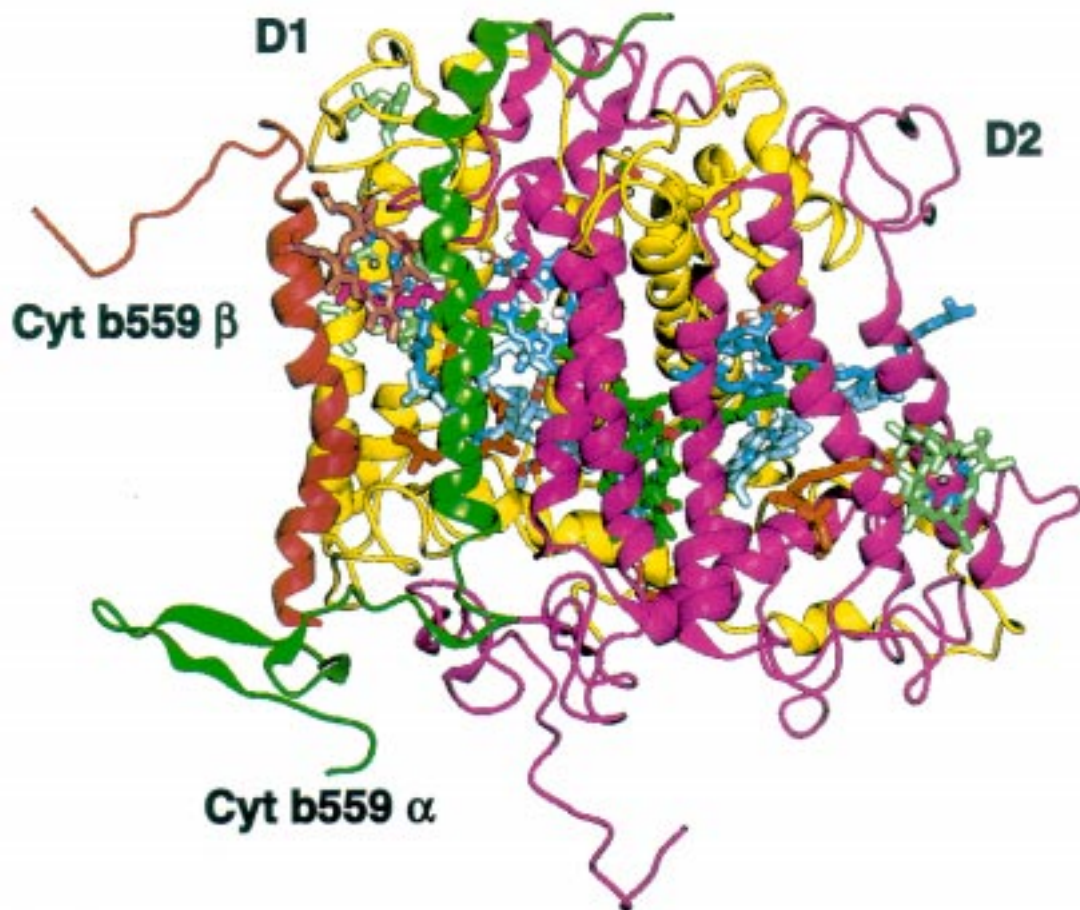


Figure 6.

Cytochrome *b559* has two subunits,  $\alpha$  and  $\beta$ , each containing one transmembrane  $\alpha$ -helical domain (Herrmann et al. 1984; Pakrasi et al. 1988) and one histidine residue which is presumably to be a heme ligand (Babcock et al. 1985). It is proposed that both histidines are required to act as ligands for the heme, which is a common situation in a number of membrane-bound *a*- and *b*-type cytochromes (Esposti 1989). Site-directed mutagenesis of the two histidines results in a complete loss of PS II (Pakrasi et al. 1991). The number of cytochrome *b559* per reaction center determined by spectroscopic and EPR analyses is one cytochrome *b559* per D1/D2 in isolated PS II preparations (Buser et al. 1992) although some favor two cytochromes. A heterodimer conformation appears to be a preferred one, consistent with the previous work of Herrmann et al. (1984) and Widger et al. (1985). Protease digestion and immuno-gold labeling experiments demonstrate that the amino terminal end of the  $\alpha$  subunit is located on the stromal side and its carboxyl end is on the luminal side (Tae et al. 1988; Vallon et al. 1989; Marr et al. 1996), and that the amino terminal end of the  $\beta$  subunit is located on the stromal end (Tae and Cramer 1994). If the heme is coordinated by the histidines from each subunit, the above data will put the heme close to the stromal end of the thylakoid membrane. The surface-enhanced Raman scattering spectroscopic data support this suggestion (Picorel et al. 1994). Although the estimate for the number of hemes per reaction center has been a matter of controversy in the literature (Whitmarsh and Pakrasi 1996), in isolated reaction center preparations, the stoichiometry for the  $\alpha$  and  $\beta$  subunits is 1:1 (Widger et al. 1985), and that for D1, D2, and cytochrome *b559* is 1:1:1 (Nanba and Satoh 1987). The heme group can also exist in at least two different interconvertible redox potential forms, a pH-independent high potential form and a pH-dependent low potential form (Whitmarsh and Pakrasi 1996). Shuvalov (1994) has proposed a model that allows a hydroxyl anion binding between the heme iron and the  $\epsilon$ 2-nitrogen of the histidine of the  $\alpha$  subunit in

the  $\alpha/\beta$  heterodimer form, making it a low potential (or extra low potential) form of cytochrome *b559*. A modeling result of the heme moiety of the cytochrome was presented by Nugent (1996).

In this minireview, we suggest a conformation that accommodates the consensus of the above experimental data. We have modeled one cytochrome *b559* with the  $\alpha/\beta$  form (the amino acid sequences were based on Mor et al. 1995). The cytochrome was positioned with the N-terminal ends of both subunits on the stromal side and C-terminal ends on the luminal side and was placed near the D1/D2 complex fitting into the open space between the two proteins (Figure 2). This location appears to match the electron projection map of the two dimensional PS II crystal structure (Nakazato et al. 1996). Transmembrane  $\alpha$ -helices of the  $\alpha$  and  $\beta$  subunits were assigned according to the sequence analyses of Cramer et al. (1993) and Whitmarsh and Pakrasi (1996). The modeling allows the heme to be liganded by specific histidines from each subunit ( $\alpha$ -H23 and  $\beta$ -H23). The conformation of the N- and C-terminal regions of the  $\alpha$  subunit and the N-terminal region for the  $\beta$  subunit was modeled using the BLAST approach. An  $\alpha$ -helix was newly generated on the N-terminal region of the  $\alpha$  subunit based on one of the searched template fragments (1NHP). Similarly, two short  $\beta$ -strands were newly generated on the C-terminus of the  $\alpha$  subunit based on the template structure of 1ALB.

The  $\alpha$  and  $\beta$  subunits together with the heme were docked in the D1/D2 complex on the  $Q_B$  side with the  $\beta$  subunit in close association with the helix E of the D1 protein. This association is based on the cross-linking experiment of Barbato et al. (1995) who suggested that the cytochrome is located on the  $Q_B$  side. In this modeling, we accommodated the above suggestion by modeling the two cross-linked regions, N-terminus of the  $\alpha$  subunit and a D1 DE loop region (D1-F239-D1-E244), in close vicinity. This contact region was suggested to play a role in photoprotective mechanism under high light. In the docking of cytochrome *b559* to the D1/D2 complex, we also took

---

←

Figure 5. The model for the binding niche of the heme in cytochrome *b559*. The heme iron is coordinated by  $\alpha$ -H23 and  $\beta$ -H23. The two propionate groups on the rings III and IV of heme are hydrogen bonded by  $\beta$ -T16 and  $\beta$ -Y12, respectively. Two tryptophan residues,  $\alpha$ -W20 and  $\beta$ -W19, appear to provide the crucial hydrophobic interactions for stabilizing the heme. (The heme that appears slightly buckled in the diagram has now been made planar in the actual file.)

Figure 6. An alternative model for cytochrome *b559*. In this model, cytochrome *b559* in the  $\alpha/\beta$  form is docked to the  $Q_A$  side of the D1/D2 complex. The  $\alpha$  subunit was modeled to be in close vicinity with the helix E of the D2 protein. The geometry of the transmembrane helix of the  $\alpha$  subunit thus resembles that of H subunit of the bacterial reaction center.

into account the following experimental evidence: the estimated distances between the heme and Q<sub>A</sub> and P680 to be 20 and 35 Å, respectively (Shuvalov 1994). The  $\alpha$  subunit is in close vicinity with the A helix of the D2 polypeptide. Mutagenesis studies of Pakrasi et al. (1991) and Shukla et al. (1992) have indicated a close association of cytochrome *b559* with the D2 polypeptide. We need to point out that the possibility of  $\alpha$  subunit being close to D1 may also exist, though our current model appears to better fit the overall electron density map of the two dimensional crystal of the Photosystem II complex (Nakazato et al. 1996).

After modeling cytochrome *b559*, we examined the protein binding region for the heme moiety. Our model in Figure 5 predicts that the heme iron is coordinated by two histidines,  $\alpha$ -H23 and  $\beta$ -H23. Both bond distances are 1.9 Å (from the Fe to the respective  $\epsilon$ 2-nitrogen of the liganding histidine residue). Two tryptophan residues,  $\alpha$ -W20 and  $\beta$ -W19, appear to provide the crucial hydrophobic interactions for stabilizing the heme. The main chain nitrogen of  $\alpha$ -W20 and sidechain of  $\beta$ -R18 provide hydrogen bonds to the two carboxylate groups on the rings III and IV of the heme, respectively. Other residues that are involved in the heme binding are  $\alpha$ -I17,  $\alpha$ -Y19,  $\alpha$ -S24,  $\alpha$ -V27,  $\alpha$ -F31 and  $\beta$ -V27. We suggest that site-directed mutagenesis on these residues be carried out to test their involvement in the heme binding.

The possibility of cytochrome *b559* being located on the Q<sub>A</sub> side is considered a valid alternative as that on the Q<sub>B</sub> side. We have thus constructed such an alternate model (Figure 6). In this alternative conformation, cytochrome *b559* in the  $\alpha/\beta$  form is docked on the Q<sub>A</sub> side of the D1/D2 complex. The  $\alpha$  subunit was modeled to be in close vicinity with the D2 protein. The location of the transmembrane helix of the  $\alpha$  subunit is thus antiparallel with the helix E of the D2 protein. The above-mentioned distance constraints were also satisfied during the modeling. It is interesting to note that in such a geometry cytochrome *b559* resembles the conformation of transmembrane part of the bacterial H subunit which functionally is involved in the assembly of the bacterial reaction center (Chory et al. 1984; Sockett et al. 1989). We propose that, in such a conformation, the transmembrane  $\alpha$ -helix of the  $\alpha$  subunit may assume a similar role by forming a nucleation center for the sequential assembly of the other components of the PS II reaction center, i.e. D1 and D2. The molecular genetic and immunological evidence provided by data of Shukla et al. (1992) and Tae and Cramer (1994) may be taken to support the notion that cytochrome *b559* may serve a functional

homologue of the H subunit in the bacterial system. It is clear that only future modeling and experimental work will provide the final answer to the location and binding of cytochrome *b559*, especially in view of the fact that we have not modeled the small molecular weight polypeptides psb I and psb W and we do not know whether that will interfere with the modelling on the Q<sub>A</sub> or the Q<sub>B</sub> side. Furthermore, even the current models of the orientation of the hemes of cytochrome *b559* are being challenged. McNamara et al. (1997) have presented data on a mutant with genetically fused subunits that suggests a model of two homodimers of  $\alpha$  and  $\beta$  subunits, with the heme in the  $\alpha$  pair facing the stroma side, and the heme in the  $\beta$  pair facing the lumen side. Although we are unable to imagine how this later idea is even feasible, the modeling work needs to be extended to see which of the current models are theoretically sustainable.

#### *Bicarbonate/water binding and transport channel*

The newly refined crystal structure of the bacterial reaction center (Ermler et al. 1994; Deisenhofer et al. 1995) shows that multiple water molecules are present to facilitate the protonation of reduced Q<sub>B</sub>. On this basis, Xiong et al. (1996) suggested an analogous water/bicarbonate binding niche which may function similarly in the D1/D2 model for the cyanobacterium *Synechocystis* 6803. Such a model was constructed by making the following assumptions: (1) Q<sub>B</sub> molecule in PS II is also buried inside the protein complex; and its protonation is ultimately dependent upon the transport of protons from the outer environment; (2) the direction of the proton transport in the PS II reaction center is similar to that in the reaction center of anoxygenic photosynthetic bacteria; (3) charged residues form the putative proton transport channel, as in the bacterial reaction center; (4) local electrostatic characteristic of the binding region weighs more than the precise geometric match with the bacterial water-binding residues; and (5) the channel to be constructed has another end at the non-heme iron site as well. Thus, by superimposing the bacterial structure (1PCR) onto the constructed PS II reaction center model, a series of D1/D2 charged residues were identified as the putative bicarbonate/water binding residues. Interestingly, most of the identified residues had been previously shown in experimental investigations to be related to the 'bicarbonate effect' (Govindjee and van Rensen 1993). A striking feature was that near the Q<sub>B</sub> and non-heme iron sites the residues are predominantly positively charged in contrast to the bacterial

reaction center which lacks the bicarbonate effect (enhancement of electron flow from reduced  $Q_A$  to singly reduced  $Q_B$ , was suggested to be due to stimulation of proton transport in PS II). In the current model that includes cytochrome *b559*, a similar attempt for constructing the channel was made based on the above assumptions. In addition to the charged D1/D2 residues, three residues from the  $\alpha$  subunit of cytochrome *b559* were also found to fall in the close vicinity of the water channel when the bacterial structure is superimposed on the PS II reaction center model. Though the inclusion of these residues can be speculative, site-directed mutagenesis on these residues is expected to provide a test of the model.

### Comparison with existing PS II reaction center models

We have presented and discussed an almost complete three dimensional model of D1–D2–cytochrome *b559* of the PS II reaction center with the inclusion of a complete set of cofactors based on homology principles as well as on experimental data, much of which were derived from site-directed mutagenesis and spectroscopic studies of the PS II reaction center. Compared to the major existing models of the PS II reaction center (see Ruffle et al. 1992; Svensson et al. 1996; Xiong et al. 1996), which have different degrees of completeness, we found the current model to have significant similarities with them as well as many differences and unique features.

It is clear that the general topology and the backbone structure of the D1 and D2 proteins of the four models from four different species (cyanobacterium *Synechocystis*; green alga *Chlamydomonas*; and the angiosperms pea and spinach) are rather similar, each with a five transmembrane  $\alpha$ -helical structure positioned symmetrically relative to the central axis of the reaction center (Svensson et al. (1996) included only four of the five D1/D2 transmembrane helices). However, due to the different alignment and energy minimization procedures used in the modeling, the length and constituents of the transmembrane  $\alpha$ -helices are slightly different in each model. The modeling of the non-transmembrane regions using the bits-and-pieces homology modeling strategy (Han and Baker 1996) in the current and in our previous model (Xiong et al. 1996) allowed us to construct the entire D1/D2 complex model which served as a basis for detailed structural analyses such as identification and analysis of interface residues (see Figure 1).

The conformations of the major cofactors common to all four models are also similar, which were derived from the bacterial counterparts, with the exception of significant modifications on the ‘special pair’ chlorophylls (Svensson et al. 1996, and this model),  $Q_A$  and  $Q_B$  (Xiong et al. 1996; this model). The important addition of chlorophyll<sub>z</sub>s,  $\beta$ -carotene on the D1 side, the tetramanganese cluster and cytochrome *b559* in this model, with the support of experimental data, extends the work beyond the scope of homology modeling and establishes a paradigm for exploitation of computer models for experimental investigation of the PS II reaction center complex.

The ligands and protein binding environment for the cofactors are of special interest in the studies of structure–function relationship of the PS II reaction center. We have thus compiled such information from the four models and show it in Table 1. In summary, the ligands to magnesium atoms of the P680 chlorophylls in all the four models are D1-H198 and D2-H197. D2-W191 appears to be a key residue that provides a ring stacking force for the reaction center chlorophyll pair P680; D1-M183 may be important in stabilizing the chlorophyll ring by providing electrostatic interactions (Svensson et al. 1996); whereas D2-T286 may provide hydrogen bonding to the ring IV of D2 P680 chlorophyll. The model of Svensson et al. (1996) also indicates the involvement of D2-S283 as well for such an interaction. The accessory chlorophylls close to the P680 chlorophylls have no histidine ligands in all the four models, whereas the chlorophyll<sub>z</sub>s, newly included in this model, are liganded by D1-H118 and D2-H117. Aromatic residues D1-F180 and D2-F179 appear to provide ring stacking forces for the accessory chlorophylls close to P680, while the D2-L206 and D2-L209 are suggested to be the ‘superexchange mediator’ for the electron transport between pheophytin and plastoquinone (Plato et al. 1989). Our previous and current models contain  $\beta$ -carotene molecule(s). The protein binding environments for  $\beta$ -carotene on the D2 side from both models are similar. The inclusion of  $\beta$ -carotene on the D1 side is new in this model. However, its modelling is considered highly tentative at this stage.

The pheophytin on the  $Q_A$  side (active side) is hydrogen bonded to the keto group on ring V by D1-E130 according to three of the four models. D1-R27 was modelled to provide such interactions in the current model. In our previous model (Xiong et al. 1996), the amide hydrogen atom of D1-Q130, as well as the hydrogen of the guanido group of D1-R27, hydrogen bond to the keto oxygen of the

Table 1. Comparison of modeling results of the binding niches of PS II cofactors from several existing models of the PS II reaction center. NS: information not explicitly stated in the paper; the table is not from a comparison of the actual models

Cofactors	Proposed structural role	Residues ( <i>C. reinhardtii</i> model) This paper	Residues ( <i>Synechocystis</i> 6803 model) Xiong et al. (1996)	Residues (spinach model) Svensson et al. (1996)	Residues (pea model) Ruffle et al. (1992)
Chlorophyll special pair	Ligands to magnesiums	D1-H198 and D2-H197	D1-H198 and D2-H197	D1-H198 and D2-H198	D1-H198 and D2-H198
	Provide ring stacking forces	D2-W191	D2-W191.	D2-W192	NS
	H-bond to the ester group on the ring IV of D2 P680 chlorophyll	D1-T286	NS	D1-T286 and D2-S283	NS
	Electrostatic interactions	D1-M183	D1-M183	D1-M184	NS
Accessory chlorophylls	Ligands to magnesiums	D1-H118 and D2-H117 (for chlorophyll <sub>z</sub> )	NS	NS	NS
	Provide ring stacking forces	D1-F180 and D2-F179	D1-F180 and D2-F179	NS	–
	Serve as a conduit for electron transport between the accessory chlorophyll and the active pheophytin on the Q <sub>A</sub> side	D2-L205 and D2-L209	D2-L205	NS	D2-L206
$\beta$ -Carotene (D2 side)	Form the binding pocket	D2-A44, D2-L45, D2-W48, D2-L49, D2-T51, D2-Y67, D2-L74, D2-F91, D2-W111, D2-A112, D2-A115, D2-A119, D2-L116, D2-F153, D2-V156, D2-F157, D2-W167, D2-P171, D2-S172, D2-F173, D2-G174, D2-V175 and D2-I178	D2-L45, D2-W48, D2-L49, D2-A71, D2-L74, D2-F91, D2-W111, D2-D112, D2-F113, D2-A115, D2-A119, D2-L116, D2-F153, D2-V154, D2-F157, D2-L158, D2-S172, D2-F173, D2-G174, and D2-V175	NS	NS
$\beta$ -Carotene (D1 side)	Form the binding pocket	D1-F48, D1-R64, D1-E65, D1-P66, D1-Y112, D1-Q113, D1-L114, D1-I115, D1-V116, D1-C117, D1-F119, D1-L120, D1-L121, D1-A154,	NS	NS	NS

Table 1. Continued

Cofactors	Proposed structural role	Residues ( <i>C. reinhardtii</i> model) This paper	Residues ( <i>Synechocystis</i> 6803 model) Xiong et al. (1996)	Residues (spinach model) Svensson et al. (1996)	Residues (pea model) Ruffle et al. (1992)
		D1-F158, D1-L174, D1-G175, D1-I176, D1-T179, and D1-F180			
Pheophytin (active side)	H-bond to the keto group on ring V	D1-R27	D1-R27 and D1-Q130	D1-E130	D1-E130
Pheophytin (active side, continued)	H-bond to ester group of the ring IV	D1-Y126	D1-Y147	D1-Y147/D1-Y126	D1-Y126
	Provide ring stacking for pheophytin	D1-Y147	D1-Y147	NS	NS
	H-bond to ester oxygen of phytol branch	NA	D1-Y126	NS	NS
	Serve as a conduit for electron transport between the active pheophytin and Q <sub>A</sub>	D2-W253 and D2-I213	D2-W253 and D2-I213	D1-I143 and D2-I214	D2-W254
Pheophytin (inactive side)	H-bond to the keto group on ring V	D2-Q129 and D2-N142	D2-Q129 and D2-N142	D2-Q130 and D2-Q143	D2-Q130
	Provide ring stacking forces	D2-F146	D2-F146	D2-F147	NS
	Located between the inactive pheophytin and Q <sub>B</sub> function unknown	D1-F255 and D1-M214	D1-F255 and D1-M214	D1-M214	NS
Q <sub>A</sub>	H-bond to the carbonyl oxygens	D2-H214 and D2-S262	D2-T217, D2-N230, D2-S262 and D2-N263	NS (not included in the model)	NS
	Form the binding pocket	D2-G206, D2-H214, D2-T217, D2-V218, D2-A249, D2-N250, D2-W253, D2-N263, D2-K264, D2-L267, D2-L209, D2-L210, D2-I213, D2-Q255, D2-V259, D2-A260, D2-F261, D2-S262, and D2-F270	D2-H214, D2-T217, D2-T221, D2-N230, D2-A249, D2-N250, D2-W253, D2-S254, D2-S262, D2-N263, D2-K264, D2-L267, D2-L209, D2-L210, D2-I213, D2-Q255, D2-I259, D2-A260, D2-F261, and D2-W266	NS (not included in the model)	D2-L211, D2-I214, D2-H215, D2-T218, D2-M247, D2-A250, D2-W254, D2-F262, D2-N264, D2-K265, and D2-L268
	Ring stack with Q <sub>A</sub>	D2-W252	D2-W252	NS (not included in the model)	NS

Table 1. Continued

Cofactors	Proposed structural role	Residues ( <i>C. reinhardtii</i> model) This paper	Residues ( <i>Synechocystis</i> 6803 model) Xiong et al. (1996)	Residues (spinach model) Svensson et al. (1996)	Residues (pea model) Ruffle et al. (1992)
Q <sub>B</sub>	H-bond to the carbonyl oxygens	D1-H215 and D1-H252	D1-H215, D1-H252 and D1-S264	NS (not included in the model)	D1-S264
	Form the binding pocket	D1-H215, D1-L218, D1-V219, D1-F246, D1-A251, D1-H252, D1-F255, D1-I259, D1-S264, D1-N267, D1-S268, D1-L271, D1-P196, D1-F197, D1-L200, D1-A203, D1-G207, D1-F211, D1-M214, D1-A263, D1-F265, D1-W278, D1-I281, D1-F285, and D2-I231	D1-H215, D1-V219, D1-Y246, D1-A251, D1-H252, D1-F255, D1-S264, D1-N266, D1-L271, D2-F232, D1-F211, D1-M214, D1-I259, D1-F260, D1-Y262, D1-A263, D1-F265, D2-I30, D2-L37, D2-F38, D2-F125, and D2-R128	NS (not included in the model)	D1-F211, D1-M214, D1-H215, D1-L218, D1-V219, D1-A251, D1-H252, D1-F255, D1-I259, D1-Y262, D1-S264, D1-N266, D1-N267, D1-S268, and D1-L271
Non-heme iron	Ligands to the iron	bicarbonate, D1-H215, D1-H252, D2-H214, and D2-H268	bicarbonate, D1-H215, D1-H272, D2-H214, and D2-H268	D1-H215, D1-H272, D2-H215, and D2-H269	D1-E231, D1-H215, D1-H272, D2-H215, and D2-H269
Bicarbonate at the non-heme iron	Form the binding pocket	D1-I224, D1-V219, D1-D227, D1-S258, D2-G226, D2-R233, D2-A234, and D2-Q239	D1-L233, D1-V219, D2-N230, D2-F232, D2-R233, D2-A234, D2-P237 and D2-K264	NS (not included in the model)	NS
Donor Z	Located between Z and P680	D1-A156, D1-V157, D1-F186, D1-G289, D1-L290, and D1-T292	D1-A156, D1-F186, D1-A287, D1-M288, D1-G289, D1-V290, D1-S291, D1-T292, and D1-M293	For details, see the paper	D1-V157, D1-F182, D1-V185, D1-F186, and D1-I289
	Surrounding protein environment	D1-S155, D1-A156, D1-V157, D1-F158, D1-L159, D1-V160, D1-P162, D1-I163, D1-G164, D1-Q165, D1-G166, D1-D170, D1-H190, D1-L290, D1-T292, D1-M293, D1-A294, and D1-F295	D1-T155, D1-V157, D1-F158, D1-L159, D1-I160, D1-P162, D1-I163, D1-G164, D1-Q165, D1-G166, D1-N298, D1-G299, D1-N301, D1-N303, and D1-Q304	D1-Q165, D1-D170, D1-F186, D1-Q189, and D1-A294	D1-P162, D1-Q165, D1-D170, D1-G171, D1-F182, D1-F186, D1-H190, and D1-I290
	Electrostatic interactions	NS	NS	D1-H190	NS
Donor D	Surrounding protein environment	D2-H87, D2-V154, D2-S155, D2-V156,	D2-V154, D2-S155, D2-V156, D2-F157,	D2-F170, D2-F182, D2-F189, D2-L290,	D2-P162, D2-Q165, D2-F170, D2-F182,

Table 1. Continued

Cofactors	Proposed structural role	Residues ( <i>C. reinhardtii</i> model) this paper	Residues ( <i>Synechocystis</i> 6803 model) Xiong et al. (1996)	Residues (spinach model) Svensson et al. (1996)	Residues (pea model) Ruffle et al. (1992)
		D2-F157, D2-L158, D2-I159, D2-P161, D2-L162, D2-Q164, D2-F169, D2-F185, D2-H189, D2-V286, D2-V287, and D2-L289	D2-L158, D2-M159, D2-P161, D2-L162, D2-G163, D2-Q164, D2-F169, D2-A170, D2-D171, D2-F185, D2-A290, D2-L291, and D2-N292	and D2-A2901	D2-F186, D2-H190, D-W192, and D2-L294
	Provide H-bonding	D2-H189	D2-F169 (backbone)	D2-H190 and D2-Q165	D2-H190 and D2-Q165
Tetramanganese cluster, Ca, and Cl	Ligands to Mn/Ca/Cl	D1-D170, D1-E189, D1-H337, D1-D342, and D1-A344	NS (not included in the model)	NS (not included in the model)	NS (not included in the model)
	Form the Mn binding pocket	D1-L91, D1-D170, D1-F182, D1-E189, D1-H190, D1-M293, D10N296, D1-N301, D1-A336, D1-H227, D1-N338, D1-F339, F1-P340, D1-L341, D1-D342, D1-L343, and D1-A344	NS (not included in the model)	NS (not included in the model)	NS (not included in the model)
Bicarbonate/water	Form the putative transport channel (with cytochrome b559 modeled at the QB side)	D1-K238, D1-E242, D1-E243, D1-E244, D1-H252, D1-R257, D1-R269, D2-R23, D2-D25, D2-D227, D2-R233, D2-E242, D2-K254, D2-R26, Cyt $\alpha$ -K3, cyt $\alpha$ -E6 and Cyt $\alpha$ -R7	D1-H215, D1-K238, D1-E242, D1-E243, D1-E244, D1-H252, D1-R257, D1-R269, D2-K23, D2-D25, D2-E224, D2-R233, D1-E236, D2-E241, D2-E242, D2-K264, and D2-R265	NS (not included in the model)	NS (not included in the model)
Heme of cytochrome b559	Ligands to the heme iron	$\alpha$ -H23 and $\beta$ -H23	NS (not included in the model)	NS (not included in the model)	NS (not included in the model)
	Form the binding pocket	$\alpha$ I17, $\alpha$ Y19, $\alpha$ -W20, $\alpha$ -S24, $\alpha$ -V27, $\alpha$ -F31, $\beta$ -R18, $\beta$ -W19, and $\beta$ -V27	NS (not included in the model)	NS (not included in the model)	NS (not included in the model)

pheophytin molecule. However, in *C. reinhardtii*, D1-130 is a glutamate instead. We assume that this is in

an acidic carboxylate ( $-\text{COO}^-$ ) form. Different conclusions would be obtained if this was not the case.

Though the sidechain of this residue and the keto oxygen of the pheophytin, both being electron negative, were sufficiently close in our initial raw model *before* energy minimization, they were moved further apart from each other after the structural refinement which removed the unfavorable interactions (in our model,  $\epsilon 2$  hydroxyl oxygen (O3) of active pheophytin (on D1) is 4.9 Å from O $\epsilon 2$  of glutamic acid-130, whereas the distance from O $\epsilon 1$  of glutamate is 5.6 Å). The nearby D1-R27 with its basic guanido group thus provides the only interaction with the keto oxygen (the distances in our current model from the oxygen of active pheophytin to NH1 are 3, to NH2 4.6 and to N epsilon 4.6 Å of the arginine residue). However, the residue is still within reasonable close vicinity of the pheophytin oxygen. Site-directed mutagenesis in *Synechocystis* 6803 changing this residue from glutamine into a glutamate caused the difference absorption spectrum to shift 3 nm and resemble the spectrum of the higher plants, the pheophytins of which have a higher quantum yield efficiency (Giorgi et al. 1996). This may suggest that in reality either this interaction between D1-130 and pheophytin is not needed for high efficiency or the sidechain of D1-E130 exists in a protonated form which may provide a stronger interaction or a water molecule may be bound in between the pheophytin oxygen and the carboxylate group of D1-E130. Any of the above three possibilities will need further experimental tests. The ester group of the ring IV of the pheophytin is hydrogen bonded by D1-Y126 and/or D1-Y147. However, the model of Xiong et al. (1996) suggests that D1-Y147 ring stacks with pheophytin while D1-Y126 hydrogen bonds to the ester oxygen in the phytol branch. We note that the template structure of the cofactors used in the previous model was that of *R. viridis* (1PRC), whereas that used in this paper is *R. sphaeroides* (1PCR). The variations are more prominent in the phytol branches for the bacteriochlorophylls and bacteriopheophytins, and thus affecting the modeling results. D2-W253, D2-I213, and perhaps D2-I143, are considered 'conduit residues' which are located between the pheophytin and the Q<sub>A</sub> head group. More consensus in modelling is found for the pheophytin in the inactive side with D2-Q129, D2-N142 hydrogen bonding to the keto group on the ring V, and D2-F146 providing the ring stacking force to the porphyrin ring. Due to the manipulation of Q<sub>A</sub> in this model, more differences are found for the Q<sub>A</sub> binding pocket. In this model, the carbonyl oxygens of Q<sub>A</sub> are hydrogen bonded by D2-H214 and D2-S262, one on each side; whereas in our previous model (Xiong et al. 1996) D2-T217,

D2-N230, D2-S262 and D2-N263, two on each side, provided hydrogen bonding to Q<sub>A</sub>. The rest of the Q<sub>A</sub> binding pocket, both for the head group and the phytol tail, is also different in the two models. However, in both our models, D2-W252 ring stacks with Q<sub>A</sub>. Ruffle et al. (1992) had only modeled the Q<sub>A</sub> head group and thus had less residues in its binding pocket, while the model of Svensson et al. (1996) lacks the plastoquinones, Q<sub>A</sub> and Q<sub>B</sub>. In the current model as well as in our previous model, Q<sub>B</sub> is hydrogen bonded by D1-H215, D1-H252 and/or D1-S264, whereas the model of Ruffle et al. (1992) indicates only D1-S264 to be the hydrogen bonding residue. Further computational work by Mackay and O'Malley (1993a, b) on the model of Ruffle et al. (1992) confirmed their results on the quinone and herbicide binding sites. Since significant manual manipulation was also involved for modeling Q<sub>B</sub> in the current study, it has resulted in some differences in residues forming the Q<sub>B</sub> binding pocket. The non-heme iron is modeled to be liganded by four conserved histidine residues, D1-H215, D1-H272, D2-H214, D2-H268 and a bicarbonate anion. The bicarbonate binding environment is also slightly different from that in the previous model (Xiong et al. 1996).

The model of Svensson et al. (1996) differs from that of Ruffle et al. (1992) and Xiong et al. (1996, this paper). In the Svensson et al. model, D1-H190 is a key residue in electrostatic interaction with the donor Z; and in the Ruffle et al. model (as well as in both our PS II models), it is not. On the other hand, D2-H189 is hydrogen bonded to the donor D in all models, but it has a stronger interaction in the Svensson et al. model compared to the Xiong et al. models. The amino acid ligands in the tetramanganese center and the binding pocket for the heme iron in cytochrome *b559* are unique in our current model and have been described above. The residues forming the putative water/bicarbonate transport channel are rather similar in both the current and in our previous model (Xiong et al. 1996) with the tentative inclusion of several cytochrome *b559* residues in our newer model.

### Concluding remarks

In summary, through the comparison of the key residues associated with the cofactors in the four major models, a consensus of the modeling results can be drawn and further experimentation can be designed to test the validity or resolve inconsistencies between the models. It needs to be further emphasized, however,

that the construction of the current PS II model, for this minireview, which has touched many areas in the research of PS II structure and function is based on several lines of experimental evidence, some of which are still controversial. Thus our model and others discussed above are by no means to be considered *real* structures. The tentative nature of the predictions and hypotheses made on the PS II reaction center structure is fully recognized by the authors and will certainly be subjected to future experimental verifications. We await the crystal structure of the PS II to validate or reject the various parts of our model.

### Acknowledgments

We dedicate this Minireview to two dear and respected pioneers, Professors Achim Trebst (of Bochum, Germany) and Mel Klein (of Berkeley, CA, USA). We thank Dr John Whitmarsh for discussions. We are indebted to Dr. Bengt Svensson for discussions as well as critical comments on our models. The work was initiated with the support of an NSF grant (91-16838, supplement 1994) and a University of Illinois Research Board grant to G. J.X. was supported by a training grant (NSF, DBI 96-02240) from the Triagency (DOE/NSF/USDA) Program for Collaborative Research in Plant Biology. G thanks the University of Illinois for sabbatical leave during 1996–1997 when this work was completed. The computational resources were provided by the National Center for Supercomputing Applications.

### References

- Allakhverdiev SI, Klimov VV and Demeter S (1992) Thermoluminescence evidence for light-induced oxidation of tyrosine and histidine residues in manganese-depleted Photosystem II particles. *FEBS Lett* 297: 51–54
- Altschul SF, Gish W, Miller W, Myers EW and Lipman DJ (1990) Basic local alignment search tool. *J Mol Biol* 215: 403–410
- Astashkin AV, Kodera Y and Kawamori A (1994) Distance between tyrosines Z(+) and D<sup>+</sup> in plant Photosystem II as determined by pulsed EPR. *Biochim Biophys Acta* 1187: 89–93
- Astashkin AV, Mino, H, Kawamori, A and Ono, T-A (1997) Pulsed EPR study of the S<sub>3</sub><sup>1</sup> signal in the Ca<sup>2+</sup>-depleted Photosystem II. *Chem Phys Lett* 272: 506–516
- Babcock GT (1995) The oxygen-evolving complex in Photosystem II as a metallo-radical enzyme. In: P. Mathis (ed) *Photosynthesis: From Light to Biosphere*, Vol II, pp 209–215. Kluwer Academic Publishers, Dordrecht, The Netherlands
- Babcock GT, Widger WR, Cramer WA, Oertling WA and Metz JG (1985) Axial ligands of chloroplast cytochrome *b*-559: Identification and requirement for a heme-cross-linked polypeptide structure. *Biochemistry* 24: 3638–3645
- Barbato R, Friso G, Ponticos M and Barber J (1995) Characterization of the light-induced cross-linking of the  $\alpha$ -subunit of cytochrome *b559* and the D1 protein in isolated Photosystem II reaction centers. *J Biol Chem* 270: 24032–24037
- Barber J, Chapman DJ and Telfer A (1987) Characterization of a PS II reaction centre isolated from the chloroplasts of *Pisum sativum*. *FEBS Lett* 220: 67–73
- Barber J, Nield J, Morris EP, Zheleva D and Hankamer B (1997) The structure, function and dynamics of photosystem two. *Physiol Plant* 100: 817–827
- Berthomieu C and Boussac A (1995) Histidine oxidation in the S<sub>2</sub> to S<sub>3</sub> transition probed by FTIR difference spectroscopy in the Ca<sup>2+</sup>-depleted Photosystem II: Comparison with histidine radicals generated by UV irradiation. *Biochemistry* 34: 1541–1548
- Bialek-Bylka GE, Tomo T, Satoh K and Koyama Y (1995) 15-*Cis*- $\beta$ -carotene found in the reaction center of spinach Photosystem II. *FEBS Lett* 363: 137–140
- Bialek-Bylka GE, Hiyama T, Yumoto K and Koyama Y (1996) 15-*cis*- $\beta$ -carotene found in the reaction center of spinach Photosystem I. *Photosynth Res* 49: 245–250
- Blankenship R and Sauer K (1974) Manganese in photosynthetic oxygen evolution. Electron paramagnetic resonance study of the environment of Mn in Tris-washed chloroplasts. *Biochim Biophys Acta* 357: 252–266
- Bögershausen O, Haumann M and Junge W (1996) Photosynthetic oxygen evolution: H/D isotope effects and the coupling between electron and proton transfer during transitions S<sub>2</sub> to S<sub>3</sub> and S<sub>3</sub> to S<sub>4</sub> and S<sub>0</sub>. *Ber Bunsenges Phys Chem* 100: 1987–1992
- Bowlby NR, Sithole I, Babcock GT and McIntosh L (1996) Potential metal ligands in photosynthetic water oxidation identified by site-directed mutagenesis of *Synechocystis* sp. PCC 6803. *Ber Bunsenges Phys Chem* 100: 1978–1986
- Bowyer J, Hilton JM, Whitelegge J, Jewess P, Camilleri P, Crofts A and Robinson H (1990) Molecular modelling studies on the binding of phenylurea inhibitors to the D1 protein of Photosystem II. *Z Naturforsch* 45c: 379–387
- Britt RD (1996) Oxygen evolution. In: Ort DR and Yocum CF (eds) *Oxygenic Photosynthesis: The Light Reactions*, pp 137–164. Kluwer Academic Publishers, Dordrecht, The Netherlands
- Brooks BR, Bruccoleri RE, Olafson BD, States DJ, Swaminathan S, Karplus M (1983) CHARMM: A program for macromolecular energy, minimization, and dynamics calculations. *J Comput Chem* 4: 187–217
- Buser CA, Diner BA and Brudvig GW (1992) Reevaluation of the stoichiometry of cytochrome *b559* in Photosystem II and thylakoid membranes. *Biochemistry* 31: 11441–11448
- Campbell KA, Peloquin JM, Diner, BA, Tang X-S, Chisholm DA and Britt RD (1997) The  $\tau$ -nitrogen of D2 histidine 189 is the hydrogen bond donor to the tyrosine radical Y<sub>D</sub> of Photosystem II. *J Am Chem Soc* 119: 4787–4788
- Chang HC, Jankowiak R, Reddy NRS, Yocum CF, Picorel R, Seibert m and Small GJ (1994) On the question of the chlorophyll *a* content of the Photosystem II reaction center. *J Phys Chem* 98: 7725–7735
- Chory J, Donohue TJ, Warga AR, Staehelin LA and Kaplan S (1984) Induction of the photosynthetic membranes of *Rhodospseudomonas sphaeroides*: Biochemical and morphological studies. *J Bacteriol* 159: 540–554
- Chu H-A, Nguyen AP and Debus RJ (1995) Amino acid residues that influence the binding of manganese or calcium to Photosystem II. 2. The carboxy-terminal domain of the D1 polypeptide. *Biochemistry* 34: 5859–5882

- Coleman WJ and Govindjee (1987) A model for the mechanism of chloride activation of oxygen evolution in Photosystem II. *Photosynth Res* 13: 199–223
- Cramer WA, Tae G-S, Furbacher PN and Böttger M (1993) The enigmatic cytochrome *b*-559 of oxygenic photosynthesis. *Physiol Plant* 88: 705–711
- Dau H, Andrews JC, Roelofs TA, Latimer MJ, Liang W, Yachandra VK, Sauer K and Klein MP (1995) Structural consequences of ammonia binding to the manganese center of the photosynthetic oxygen-evolving complex: An X-ray absorption spectroscopy study of isotropic and oriented Photosystem II particles. *Biochemistry* 34: 5274–5287
- Debus RJ (1992) The manganese and calcium ions of photosynthetic oxygen evolution. *Biochim Biophys Acta* 1102: 269–352
- Deisenhofer J, Epp O, Sinning I and Michel H (1995) Crystallographic refinement at 2.3-Å resolution and refined model of the photosynthetic reaction centre from *Rhodospseudomonas viridis*. *J Mol Biol* 246: 429–457
- De Las Rivas J, Telfer A and Barber J (1993) Two coupled  $\beta$ -carotene molecules protect P680 from photodamage in isolated Photosystem II reaction centres. *Biochim Biophys Acta* 1142: 155–164
- Depka B, Jahns P and Trebst A (1998)  $\beta$ -carotene to zeaxanthin conversion in the rapid turnover of the D1 protein of Photosystem II. *FEBS Lett* 424: 267–274
- Diner BA and Babcock GT (1996) Structure, dynamics, and energy conversion efficiency in Photosystem II. In: Ort DR and Yocum CF (eds) *Oxygenic Photosynthesis: The Light Reactions*, pp 213–247. Kluwer Academic Publishers, Dordrecht, The Netherlands
- Eijkkelhoff C and Dekker JP (1995) Determination of the pigment stoichiometry of the photochemical reaction center of Photosystem II. *Biochim Biophys Acta* 1231: 21–28
- Eijkkelhoff C, Vacha F, van Grondelle R, Dekker J and Barber J (1997) Spectroscopic characterization of a 5 Chl *a* Photosystem II reaction center complex. *Biochim Biophys Acta* 1318: 266–274
- Erickson JM, Rahire M and Rochaix J-D (1984) *Chlamydomonas reinhardtii* gene for the 32,000 mol. wt. protein of Photosystem II contains four large introns and is located entirely within the chloroplast inverted repeat. *EMBO J* 3: 2753–2762
- Erickson JM, Rahire M, Malnoe P, Girard-Bascou J, Pierre Y, Benoun P and Rochaix J-D (1986) Lack of the D2 protein in a *Chlamydomonas reinhardtii psbD* mutant affect Photosystem I stability and D1 protein. *EMBO J* 5: 1745–1754
- Ermiler U, Fritsch G, Buchanan SK and Michel H (1994) Structure of the photosynthetic reaction centre from *Rhodobacter sphaeroides* at 2.65 Å resolution: Cofactors and protein-cofactor interactions. *Structure* 2: 925–936
- Esposti MD (1989) Prediction and comparison of the haem-binding sites in membrane haemproteins. *Biochim Biophys Acta* 977: 249–265
- Fowler CF and Kok B (1974) Proton evolution associated with the photooxidation of water in photosynthesis. *Biochim Biophys Acta* 357: 299–307
- Frank HA, and Cogdell RJ (1996) Carotenoids in photosynthesis. *Photochem Photobiol* 63: 257–264
- Fujiwara M, Hayashi H, Tasumi M, Kanaji M, Koyama Y, and Satoh K (1987) Structural studies on a Photosystem II reaction center complex consisting of D-1 and D-2 polypeptides and cytochrome *b*-559 by resonance Raman and high-performance liquid chromatography. *Chem Lett* 10: 2005–2008
- Gilchrist ML, Ball J Jr, Randall DW and Britt RD (1995) Proximity of the manganese cluster of Photosystem II to the redox-active tyrosine  $Y_Z$ . *Proc Natl Acad Sci USA* 92: 9545–9549
- Giorgi LB, Nixon PJ, Merry SAP, Joseph DM, Durrant JR, De Las Rivas J, Barber J, Porter G and Klug DR (1996) Comparison of primary charge separation in the Photosystem II reaction center complex isolated from wild-type and D1-130 mutants of the cyanobacterium *Synechocystis* PCC 6803. *J Biol Chem* 271: 2093–2101
- Govindjee and Van Rensen JJS (1993) Photosystem II reaction center and bicarbonate. In: Deisenhofer J and Norris J (eds) *The Photosynthetic Reaction Center*, Vol I, pp 357–389. Academic Press, San Diego, CA
- Greenfield SR, Seibert M, Govindjee and Wasielewski MR (1997) Direct measurement of the effective rate constant for primary charge separation in isolated Photosystem II reaction centers. *J Phys Chem* 101: 2251–2255
- Gounaris K, Chapman DJ, Booth P, Crystall B, Giorgi LB, Klug DR, Porter G and Barber J (1990) Comparison of D1/D2/cytochrome *b*559 reaction centre complex of photosystem two isolated by two different methods. *FEBS Lett* 265: 88–92
- Han KF and Baker D (1996) Global properties of the mapping between local amino acid sequence and local structure in proteins. *Proc Natl Acad Sci USA* 93: 5814–5818
- Hankamer B, Barber J and Boekema EJ (1997) Structure and membrane organization of Photosystem II in green plants. *Annu Rev Plant Physiol Plant Mol Biol* 48: 641–671
- Hara H, Kawamori A, Astashkin AV and Ono T (1996) The distances from tyrosine D to redox-active components on the donor side of Photosystem II determined by pulsed electron-electron double resonance. *Biochim Biophys Acta* 1276: 140–146
- Hara H, Dzuba SA, Kawamori A, Akabori K, Tomo T, Satoh K, Iwaki M and Itoh S (1997) The distance between P680 and QA in Photosystem II determined by ESSEM spectroscopy. *Biochim Biophys Acta* 1322: 77–85
- Haumann M, Hundelt M, Drenstedt W and Junge M (1996) Photosystem II of green plants. Oxidation and deprotonation of the same component (histidine?) on  $S_1^* \bullet S_2^*$  in chloride-depleted centers as on  $S_2 \bullet S_3$  in controls. *Biochim Biophys Acta* 1273: 237–250
- Haumann M, Mulkidjanian A and Junge W (1997a) Electrogenicity of electron and proton transfer at the oxidizing side of Photosystem II. *Biochemistry* 36: 9304–9315
- Haumann M, Bögershausen O, Cherepanov D, Ahlbrink R and Junge W (1997b) Photosynthetic oxygen evolution: H/D isotope effects and the coupling between electron and proton transfer during the redox reactions at the oxidizing side of Photosystem II. *Photosyn Res* 51: 193–208
- Herrmann RG, Alt J, Schiller B, Widger WR and Cramer WA (1984) Nucleotide sequence of the gene for apocytochrome *b*559 on the spinach plastid chromosome: Implications for the structure of the membrane proteins. *FEBS Lett* 176: 239–244
- Herrmann RG, Oelmüller R, Bichler J, Schneiderbauer A, Steppuhn J, Wedel N, Tyagi AK and Westhoff P (1991) The thylakoid membrane of higher plants: Genes, their expression and interaction. In: Herrmann RG and Larkins BA (eds) *Plant Molecular Biology*, Vol 2, pp 411–427. Plenum, New York
- Hofmann E, Wrench PM, Sharples FP, Hiller RG, Welte W and Diederichs K (1996) Structural basis of light harvesting by carotenoids: Peridinin-chlorophyll-protein from *Amphidinium carterae*. *Science* 272: 1788–1791
- Hoganson CW and Babcock GT (1989) Redox cofactor interactions in Photosystem II: Electron spin resonance spectrum of  $P_{680}^+$  is broadened in the presence of  $Y_Z^+$ . *Biochemistry* 28: 1448–1454
- Hundelt M, Haumann M, and Junge W (1997) Cofactor X of photosynthetic water oxidation: Electron transfer, proton release, and electrogenic behaviour in chloride-depleted Photosystem II. *Biochim Biophys Acta* 1321: 47–60

- Hutchison RS and Sayre RT (1995) Site-specific mutagenesis at histidine 118 of the Photosystem II D1 protein of *Chlamydomonas reinhardtii*. In: Mathis P (ed) Photosynthesis: From Light to Biosphere, Vol 1, pp 471–474. Kluwer Academic Publishers, Dordrecht, The Netherlands
- Karge M, Irgang KD and Renger G (1997) Analysis of the reaction coordinate of photosynthetic water oxidation by kinetic measurements of 355 nm absorption changes at different temperatures in Photosystem II preparations suspended in either H<sub>2</sub>O or D<sub>2</sub>O. *Biochemistry* 36: 8904–8913
- Klein MP, Sauer K and Yachandra VK (1993) Perspectives on the structure of the photosynthetic oxygen evolving manganese complex and its relation to the Kok cycle. *Photosynth Res* 38: 265–277
- Kless H and Vermaas WFJ (1996) Combinatorial mutagenesis and structural simulations in the environment of the redox active tyrosine Y<sub>Z</sub> of Photosystem II. *Biochemistry* 35: 16458–16464
- Kobayashi M, Maeda H, Watanabe T, Nakane H and Satoh K (1990) Chlorophyll *a* and b-carotene content in the D<sub>1</sub>/D<sub>2</sub>/cytochrome *b559* reaction center complex from spinach. *FEBS Lett* 260: 138–140
- Kodera Y, Dzuba SA, Hara H and Kawamori A (1994) Distance from tyrosine D<sup>+</sup> to the manganese cluster and the acceptor iron in Photosystem II as determined by selective hole burning in EPR spectra. *Biochim Biophys Acta* 1186: 91–99
- Kodera Y, Hara H, Astashkin AV, Kawamori A and Ono-TA (1995) EPR Study of trapped tyrosine Z<sup>+</sup> in Ca-depleted Photosystem II. *Biochim Biophys Acta* 1232: 43–51
- Koulougliotis D, Innes JB, and Brudvig GW (1994) Location of chlorophyll<sub>Z</sub> in Photosystem II. *Biochemistry* 33: 11814–11822
- Koulougliotis D, Tang XS, Diner BA and Brudvig GW (1995) Spectroscopic evidence for the symmetric location of tyrosines D and Z in Photosystem II. *Biochemistry* 34: 2850–2856
- Kramer DM, Roffey RA, Govindjee and Sayre RT (1994) The At thermoluminescence band from *Chlamydomonas reinhardtii* and the effects of mutagenesis of histidine residues on the donor side of the Photosystem II D1 polypeptide. *Biochim Biophys Acta* 1185: 228–237
- Krauss N, Schubert WD, Klukas O, Fromme P, Witt HT and Saenger W (1996) Photosystem I at 4 Å resolution represents the first structural model of a joint photosynthetic reaction centre and core antenna system. *Nature Struct Biol* 3: 965–973
- Kurreck J, Liu B, Napiwotzki A, Sellin S, Eckert H-J, Eichler H-J, Renger G (1997) Stoichiometry of pigments and radical pair formation under saturating pulse excitation in D1/D2/cyt *b559* preparations. *Biochim Biophys Acta* 1318: 307–315
- Kwa SLS, Newell WR, van Grondelle R and Dekker JP (1992) The reaction center of Photosystem II studied with polarized fluorescence spectroscopy. *Biochim Biophys Acta* 1099: 193–202
- Lancaster CR, Ermiler U and Michel H (1995) The structures of photosynthetic reaction centers from purple bacteria as revealed by x-ray crystallography. In: Blankenship RE, Madigan MT and Bauer CE (eds) Anoxygenic Photosynthetic Bacteria, pp 503–526. Kluwer Academic Publishers, Dordrecht, The Netherlands
- Li R, Lin N, Xu C, Shen Y and Govindjee (1997) Trichloroacetate affects redox active tyrosine 160 of the D2 polypeptide of the Photosystem II core. *Z Naturforsch* 52 C: 782–788
- Mackay SP and O'Malley PJ (1993a) Molecular modelling of the interaction between DCMU and the Q<sub>B</sub>-binding site of Photosystem II. *Z Naturforsch* 48c: 191–198
- Mackay SP and O'Malley PJ (1993b) Molecular modelling of the interactions between optically active triazine herbicide and Photosystem II. *Z Naturforsch* 48c: 474–481
- Marr KM, Mastroratte DN, and Lyon MK (1996) Two-dimensional crystals of Photosystem II: Biochemical characterization, cryo-electron microscopy and localization of the D1 and cytochrome *b559* polypeptides. *J Cell Biol* 132: 823–833
- McNamara VP, Satterwala F, Pakrasi HB and Whitmarsh J (1997) Structural model of cytochrome *b559* in Photosystem II based on a mutant with genetically fused subunits. *Proc Natl Acad Sci USA* 94: 14173–14178
- Mimuro M, Tomo T, Nishimura Y, Yamazaki I and Satoh K (1995) Identification of a photochemically inactive pheophytin molecule in the spinach D<sub>1</sub>-D<sub>2</sub>-cyt *b559* complex. *Biochim Biophys Acta* 1232: 81–88
- Montoya G, Yruela I and Picorel R (1991) Pigment stoichiometry of a newly isolated D<sub>1</sub>-D<sub>2</sub>-Cyt *b559* complex from the higher plant *Beta vulgaris*. *FEBS Lett* 283: 255–258
- Mor TS, Ohad I, Hirschberg J and Pakrasi HB (1995) An unusual organization of the genes encoding cytochrome *b559* in *Chlamydomonas reinhardtii*: *psbE* and *psbF* genes are separately transcribed from different regions of the plastid chromosome. *Mol Gen Genet* 246: 600–604
- Moskalenko AA, Barbato R and Giacomette GM (1992) Investigation of the neighbor relationships between Photosystem II polypeptides in the two types of isolated reaction centres (D1/D2/cyt**b559** and CP47/D1/D2/cyt**b559** complexes). *FEBS Lett* 314: 271–274
- Mulkidjanian AY, Cherepanov DA, Haumann M and Junge W (1996) Photosystem II of green plants: Topology of core pigments and redox cofactors as inferred from electrochromic difference spectra. *Biochemistry* 35: 3093–3107
- Nakazato K, Toyoshima C, Enami I and Inoue Y (1996) Two dimensional crystallization and cryo-electron microscopy of Photosystem II. *J Mol Biol* 257: 225–232
- Nanba O and Satoh K (1987) Isolation of Photosystem II reaction center consisting of D1 and D2 polypeptides and cytochrome *b559*. *Proc Natl Acad Sci USA* 84: 109–112
- Nixon, PJ and Diner BA (1992) Aspartate 170 of the Photosystem II reaction center polypeptide D1 is involved in the assembly of the oxygen-evolving manganese cluster. *Biochemistry* 31: 942–948
- Nixon PJ, Chisholm DA and Diner BA (1992) Isolation and functional analysis of random and site-directed mutants for Photosystem II. In: Shewry P and Gutteridge S (eds) Plant Protein Engineering, pp 93–141. Cambridge University Press, Cambridge, UK
- Noguchi T, Inoue Y and Tang X-S (1997) Structural coupling between the oxygen-evolving Mn cluster and a tyrosine residue in Photosystem II as revealed by Fourier transform infrared spectroscopy. *Biochemistry* 36: 14705–14711
- Nugent JHA (1996) Oxygenic photosynthesis. Electron transfer in Photosystem I and Photosystem II. *Eur J Biochem* 237: 519–531
- Padhye S, Kambara T, Hendrickson DN and Govindjee (1986) Manganese-histidine cluster as the functional center of the water oxidation complex in photosynthesis. *Photosynth Res* 9: 103–112
- Pakrasi HB, Williams JGK and Arntzen CJ (1988) Targeted mutagenesis of the *psbE* and *psbF* genes blocks photosynthetic electron transport: Evidence for a functional role of cytochrome *b559* in Photosystem II. *EMBO J* 7: 325–332
- Pakrasi HB, Ciechi PD and Whitmarsh J (1991) Site directed mutagenesis of the heme axial ligands of Cytochrome *b559* affects the stability of the Photosystem II complex. *EMBO J* 10: 1619–1627
- Picorel R, Chumanov G, Cotton TM, Montoya G, Toon S and Seibert M (1994) Surface-enhanced resonance Raman scattering spectroscopy of Photosystem II pigment-protein complexes. *J Phys Chem* 98: 6017–6022
- Plato M., Michel-Beyerle ME, Bixon M and Jortner J (1989) On the role of tryptophan as a superexchange mediator for quinone

- reduction in photosynthetic reaction centers. *FEBS Lett* 249: 70–74
- Pueyo JJ, Moliner E, Seibert M and Picorel R (1995) Pigment content of D1–D2-cytochrome *b559* reaction center preparations after removal of CP47 contamination: an immunological study. *Biochemistry* 34: 15214–15218
- Rhee K-H, Morris EP, Zheleva D, Hankamer B, Kühlbrandt W and Barber J (1997) Two-dimensional structure of plant Photosystem II at 8-Å resolution. *Nature* 389: 522–526
- Rigby SEJ, Heathcote P, Evans MCW and Nugent JHA (1995) ENDOR and special TRIPLE resonance spectroscopy of  $Q_A^-$  of Photosystem 2. *Biochemistry* 34: 12075–12081
- Rochaix J-D (1995) *Chlamydomonas reinhardtii* as the photosynthetic yeast. *Annu Rev Genet* 29: 209–230
- Rochaix J-D, Goldschmidt-Clermont M and Merchant S (eds) (1998) *Molecular Biology of Chlamydomonas: Chloroplasts and Mitochondria*. Kluwer Academic Publishers, Dordrecht, The Netherlands
- Roffey RA, Kramer DM, Govindjee and Sayre RT (1994) Lumenal side histidine mutations in the D1 protein of Photosystem II affect donor side electron transfer in *Chlamydomonas reinhardtii*. *Biochim Biophys Acta* 1185: 257–270
- Rögner M, Boekema EJ and Barber J (1996) How does photosystem 2 split water? The structural basis of efficient energy conversion. *TIBS* 21: 44–49
- Ruffle SV and Nugent JHA (1992) Computer modelling of the Photosystem II core proteins. In: Murata N (ed) *Research in Photosynthesis*. Vol II, pp 191–194. Kluwer Academic Publishers, Dordrecht, The Netherlands
- Ruffle SV, Donnelly D, Blundell TL and Nugent JHA (1992) A three-dimensional model of the Photosystem II reaction centre of *Pisum sativum*. *Photosynth Res* 34: 287–300
- Schelvis JPM, van Noort PI, Aartsma, TJ and van Gorkom HJ (1994) Energy transfer, charge separation and pigment arrangement in the reaction center of Photosystem II. *Biochim Biophys Acta* 1184: 242–250
- Shukla VA, Stanbekova GE, Shestakov SV and Pakrasi HB (1992) The D1 protein of the Photosystem II reaction center complex accumulates in the absence of D2: Analysis of a mutant of the cyanobacterium *Synechocystis* sp. PCC 6803 lacking cytochrome *b559*. *Mol Microbiol* 6: 947–956
- Shuvalov VA (1994) Composition and function of cytochrome *b559* in reaction centers of Photosystem II of green plants. *J Bioenerg Biomembr* 26: 619–626
- Sockett RE, Donohue TJ, Varga AR and Kaplan S (1989) Control of photosynthetic membrane assembly in *Rhodobacter sphaeroides* mediated by *puhA* and flanking sequences. *J Bacteriol* 171: 436–446
- Svensson B, Vass I, Cedergren E and Styring S (1990) Structure of donor side components in Photosystem II predicted by computer modeling. *EMBO J* 9: 2051–2059
- Svensson B, Etchebest C, Tuffery P, van Kan P, Smith J and Styring S (1996) A model for the Photosystem II reaction center core including the structure of the primary donor P-680. *Biochemistry* 35: 14486–14502
- Tae G-S and Cramer WA (1994) Topography of the heme prosthetic group of cytochrome *b-559* in the Photosystem II reaction center. *Biochemistry* 33: 10060–10068
- Tae G-S, Black MT, Cramer WA, Vallon O and Bogorad L (1988) Thylakoid membrane protein topography: transmembrane orientation of the chloroplast cytochrome *b-559 psbE* gene product. *Biochemistry* 27: 9075–9080
- Tommos C, Davidsson L, Svensson B, Madsen C, Vermaas W and Styring S (1993) Modified EPR spectra of the tyrosine $\dot{D}$  radical in Photosystem II in site-directed mutants of *Synechocystis* sp. PCC 6803: Identification of side chains in the immediate vicinity of tyrosine $\dot{D}$  on the D2 protein. *Biochemistry* 32: 5436–5441
- Trebst A (1986) The topology of the plastoquinone and herbicide binding peptides of Photosystem II – a model. *Z Naturforsch* 41c: 240–245
- Trebst A (1991) A contact site between the two reaction center polypeptides of Photosystem II is involved in photoinhibition. *Z Naturforsch* 46c: 557–562
- Trebst A and Depka B (1997) Role of carotene in the rapid turnover and assembly of Photosystem II in *Chlamydomonas reinhardtii*. *FEBS Lett* 400: 359–362
- Trebst A and Soll-Bracht E (1996) Cycloheximide retards high light driven D1 protein degradation in *Chlamydomonas reinhardtii*. *Plant Sci Lett* 115: 191–197
- Un S, Brunel L-C, Brill TM, Zimmermann J-L and Rutherford AW (1994) Angular orientation of the stable tyrosyl radical within Photosystem II by high field 245-GHz electron paramagnetic resonance. *Proc Natl Acad Sci USA* 91: 5262–5266
- Vallon O, Tae G-S, Cramer WA, Simpson D, Hoyer-Hanson G and Bogorad L (1989) Visualization of antibody binding to the photosynthetic membrane: The transmembrane orientation of cytochrome *b-559*. *Biochim Biophys Acta* 975: 132–141
- van Leeuwen PJ, Nieveen MC, van de Meent EJ, Dekker JP and van Gorkom HJ (1991) Rapid and simple isolation of pure Photosystem II core and reaction center particles from spinach. *Photosynth Res* 28: 149–153
- Vermaas WFJ, Rutherford AW and Hansson Ö (1988) Site-directed mutagenesis in Photosystem II of the cyanobacterium *Synechocystis* sp. PCC 6803; Donor D is a tyrosyl residue in the D2 protein. *Proc Natl Acad Sci USA* 85: 8477–8481
- Vermaas WFJ, Styring S, Schröder WP and Andersson B (1993) Photosynthetic water oxidation: The protein framework. *Photosynth Res* 38: 249–263
- Whitmarsh J and Pakrasi HB (1996) Form and function of cytochrome *b559*. In: Ort DR and Yocum CF (eds) *Oxygenic Photosynthesis: The Light Reactions*, pp 249–264. Kluwer Academic Publishers, Dordrecht, The Netherlands
- Widger WR, Cramer WA, Hermodson M and Herrmann RG (1985) Evidence for a hetero-oligomeric structure of the chloroplast cytochrome *b-559*. *FEBS Lett* 191: 186–190
- Xiong J, Subramaniam S and Govindjee (1996) Modeling of the D1/D2 proteins and cofactors of the Photosystem II reaction center: Implications to herbicide and bicarbonate binding. *Protein Sci* 5: 2054–2073
- Yachandra VK, Sauer K and Klein MP (1996) Manganese cluster in photosynthesis: Where plants oxidize water to dioxygen. *Chem Rev* 96: 2927–2950
- Zech SG, Kurreck J, Eckert H-J, Renger G, Lubitz W and Bittl R (1997) Pulsed EPR measurement of the distance between P680<sup>+</sup> and  $Q_A^-$  in Photosystem II. *FEBS Lett* 414: 454–456
- Zheleva D, Hankamer B and Barber J (1996) Heterogeneity and pigment composition of isolated Photosystem II reaction centers. *Biochemistry* 35: 15074–15079
- Zheng M and Dismukes GC (1996) The conformation of the isoprenyl chain relative to the semiquinone head in the primary electron acceptor ( $Q_A$ ) of higher plant PS II (plastoquinone) differs from that in bacterial reaction centers (ubiquinone or menaquinone) by ca. 90°. *Biochemistry* 35: 8955–8963